development of Fc-fusion proteins will receive further attention. Although the Fc domains are used with the intent of prolonging the half-lives of receptor proteins, the half-lives tend not to be fully prolonged to the level of IgG1. It remains unclear whether the receptor regions of Fc-fusion proteins alter the conformation of the CH2-CH3 domain interface or the regions cause steric hindrance on the binding site of FcRn; however, the molecular design of Fc-fusion proteins having a higher affinity to FcRn might be possible in either case.

Reflecting the increasing interest in the development of mAbs and related products, the newly revised guideline for such products was adopted by the European Medicines Agency in 2008 (www.emea.europa.eu/pdfs/human/bwp/15765307enfin.pdf). In the guidelines, it is mentioned that FcRn-binding activity should be provided, as appropriate, in product characterization. Because regions other than the Fc domain might affect the affinity of the protein to FcRn (Figs. 6, 7), the affinity to FcRn should be evaluated as an important quality attribute related to the pharmacokinetic profile, even if the protein has a native Fc domain of IgG1, especially in cases of Fc-fusion proteins. Meanwhile, because it was demonstrated that oxidation of two labile methionines, Met^{252} and Met^{428}, in human IgG1 attenuates binding of the Ab to FcRn (36), alteration of the affinity to FcRn during the production process or storage will reflect structural changes of the protein, including Met oxidation, that will lead to shortening the serum half-life. In addition to IgG, albumin is also known to bind to FcRn in a pH-dependent manner and is protected from degradation (37, 38). The albumin-fusion proteins (e.g., albumin-IFN) or drugs having an albumin-binding moiety are being developed. FcRn-binding characteristics would also be important as a quality attribute of such products, which is related to the pharmacokinetic profile.

As mentioned above, the existence of several Abs having a short half-life and high affinity to FcRn suggested the involvement of other critical factor(s) in regulating the serum half-life of Abs such as trastuzumab, rituximab, or infliximab. Trastuzumab is a humanized Ab directed against human epidermal growth factor receptor 2 (HER2), which is expressed in some types of breast cancer cells. It has been reported that trastuzumab is taken up by HER2-expressing cells via HER2-mediated endocytosis (39, 40). Rituximab, a chimeric Ab directed against CD20, is also internalized in an Ag-mediated manner (41). Because the ligand-dependent internalization is followed by degradation of Abs, this property seems to be an important reason for the short half-life of trastuzumab and rituximab. It has been reported that, in general, the half-life of monoclonal IgG Abs increases depending on the degree of humanization in the order of murine < chimeric < humanized < human (6, 41, 42). Because infliximab and rituximab are chimeric Abs, the involvement of common factors influencing the half-life of chimeric Abs such as the presence of human anti-chimeric Ab would be another reason for the shorter half-life.

As shown in Fig. 7, the affinities of infliximab–TNF-α complex and adalimumab–TNF-α complex seemed to be lower than those of infliximab and adalimumab. If the affinity of therapeutic proteins/target molecules complexes to FcRn is lower than that of the free therapeutic proteins, the complexes will be degraded faster. Therefore, the half-lives of such therapeutic proteins seem to be shortened in the case that the target molecules are abundant in the bodies of patients. In contrast, if the affinity to FcRn of therapeutic proteins/target molecule complexes is higher than that of the free drugs, the complexes of drug and target molecules will have longer half-lives than free drugs. Because there are many factors affecting the elimination of Abs [reviewed by Tabrizi et al. (41)], further studies are necessary to elucidate the critical factors impacting the half-lives of Fc domain-containing proteins, in addition to the affinity to FcRn. Binding characteristics of the Fc domain-containing proteins or their complex with target molecules to FcγRs would be one of the important issues to be examined in regard to the impact on their elimination.

In conclusion, we showed the importance of the affinity to FcRn in determining the serum half-life of Fc domain-containing therapeutic proteins. Further investigation regarding the molecular structures that regulate the affinity of the engineered protein to FcRn will accelerate the development of therapeutic proteins with a desired half-life.

Acknowledgments

We thank Dr. Pamela Bjorkman for the gift of the cell line expressing FcRn.

Disclosures

The authors have no financial conflicts of interest.

References

1. Morell, A., W. D. Terry, and T. A. Waldmann. 1970. Metabolic properties of IgG subclasses in man. *J. Clin. Invest.* 49: 673–680.
2. Simister, N. E., and K. E. Mostov. 1989. An Fc receptor structurally related to MHC class I antigens. *Nature* 337: 184–187.
3. Junghans, R. P., and C. L. Anderson. 1996. The protection receptor for IgG catabolism is the β_2-microglobulin-containing neonatal intestinal transport receptor. *Proc. Natl. Acad. Sci. USA* 93: 5512–5516.
4. Ghetie, V., S. Popov, J. Borvak, C. Radu, D. Matesoi, C. Medesan, R. J. Ober, and E. S. Ward. 1997. Increasing the serum persistence of an IgG fragment by random mutagenesis. *Nat. Biotechnol.* 15: 637–640.
5. Raghavan, M., V. R. Bonagura, S. L. Morrison, and P. J. Bjorkman. 1995. Analysis of the pH dependence of the neonatal Fc receptor/immunoglobulin G interaction using antibody and receptor variants. *Biochemistry* 34: 14649–14657.
6. Lobo, E. D., R. J. Hansen, and J. P. Balthasar. 2004. Antibody pharmacokinetics and pharmacodynamics. *J. Pharm. Sci.* 93: 2645–2668.
7. Datta-Mannan, A., D. R. Witcher, Y. Tang, J. Watkins, and V. J. Wroblewski. 2007. Monoclonal antibody clearance: impact of modulating the interaction of IgG with the neonatal Fc receptor. *J. Biol. Chem.* 282: 1709–1717.
8. Vaccaro, C., J. Zhou, R. J. Ober, and E. S. Ward. 2005. Engineering the Fc region of immunoglobulin G to modulate in vivo antibody levels. *Nat. Biotechnol.* 23: 1283–1288.
9. Hinton, P. R., J. M. Xiong, M. G. Johlfs, M. T. Tang, S. Keller, and N. Tsurushita. 2006. An engineered human IgG1 antibody with longer serum half-life. *J. Immunol.* 176: 346–356.
10. Dall'Acqua, W. F., P. A. Kiener, and H. Wu. 2006. Properties of human IgG1s engineered for enhanced binding to the neonatal Fc receptor (FcRn). *J. Biol. Chem.* 281: 23514–23524.
11. Petkova, S. B., S. Akilesh, T. J. Sproule, G. J. Christianson, H. Al Khabbaz, A. C. Brown, L. G. Presta, Y. G. Meng, and D. C. Roopenian. 2006. Enhanced half-life of genetically engineered human IgG1 antibodies in a humanized FcRn mouse model: potential application in humorally mediated autoimmune disease. *Int. Immunol.* 18: 1759–1769.
12. Yeung, Y. A., M. K. Leabman, J. S. Marvin, J. Qiu, C. W. Adams, S. Lien, M. A. Starovasnik, and H. B. Lowman. 2009. Engineering human IgG1 affinity to human neonatal Fc receptor: impact of affinity improvement on pharmacokinetics in primates. *J. Immunol.* 182: 7663–7671.
13. Nissim, A., and Y. Chernajovsky. 2008. Historical development of monoclonal antibody therapeutics. In *Therapeutic Antibodies (Handbook of Experimental Pharmacology)*, Vol. 181. Y. Chernajovsky and A. Nissim eds. Springer, New York, p. 3–18.
14. Reichert, J. M., C. J. Rosensweig, L. B. Faden, and M. C. Dewitz. 2005. Monoclonal antibody successes in the clinic. *Nat. Biotechnol.* 23: 1073–1078.
15. West, A. P., Jr., and P. J. Bjorkman. 2000. Crystal structure and immunoglobulin G binding properties of the human major histocompatibility complex-related Fc receptor. *Biochemistry* 39: 9698–9708.
16. Ellsworth, J. L., M. Maurer, B. Harder, N. Hamacher, M. Lantry, K. B. Lewis, S. Rene, K. Byrnes-Blake, S. Underwood, K. S. Waggie, et al. 2008. Targeting immune complex-mediated hypersensitivity with recombinant soluble human FcγRIA (CD64A). *J. Immunol.* 180: 580–589.
17. Weisman, M. H., L. W. Moreland, D. E. Furst, M. E. Weinblatt, E. C. Keystone, H. E. Paulus, L. S. Teoh, R. B. Velagapudi, P. A. Noertersheuser, G. R. Granneman, et al. 2003. Efficacy, pharmacokinetic, and safety assessment of adalimumab, a fully human anti-tumor necrosis factor-α monoclonal antibody, in adults with rheumatoid arthritis receiving concomitant methotrexate: a pilot study. *Clin. Ther.* 25: 1700–1721.
18. Vincenti, F., R. Kirkman, S. Light, G. Bumgardner, M. Pescovitz, P. Halloran, J. Neylan, A. Wilkinson, H. Ekberg, R. Gaston, et al. 1998. Interleukin-2-receptor blockade with daclizumab to prevent acute rejection in renal transplantation. *N. Engl. J. Med.* 338: 161–165.
19. Lee, H., H. C. Kimko, M. Rogge, D. Wang, I. Nestorov, and C. C. Peck. 2003. Population pharmacokinetic and pharmacodynamic modeling of etanercept using logistic regression analysis. *Clin. Pharmacol. Ther.* 73: 348–365.

20. Cornillie, F., D. Shealy, G. D'Haens, K. Geboes, G. Van Assche, J. Ceuppens, C. Wagner, T. Schaible, S. E. Plevy, S. R. Targan, and P. Rutgeerts. 2001. Infliximab induces potent anti-inflammatory and local immunomodulatory activity but no systemic immune suppression in patients with Crohn's disease. *Aliment. Pharmacol. Ther.* 15: 463–473.
21. Hooks, M. A., C. S. Wade, and W. J. Millikan, Jr. 1991. Muromonab CD-3: a review of its pharmacology, pharmacokinetics, and clinical use in transplantation. *Pharmacotherapy* 11: 26–37.
22. Casale, T. B., I. L. Bernstein, W. W. Busse, C. F. LaForce, D. G. Tinkelman, R. R. Stoltz, R. J. Dockhorn, J. Reimann, J. Q. Su, R. B. Fick, Jr., and D. C. Adelman. 1997. Use of an anti-IgE humanized monoclonal antibody in ragweed-induced allergic rhinitis. *J. Allergy Clin. Immunol.* 100: 110–121.
23. Subramanian, K. N., L. E. Weisman, T. Rhodes, R. Ariagno, P. J. Sánchez, J. Steichen, L. B. Givner, T. L. Jennings, F. H. Top, Jr., D. Carlin, and E. Connor. 1998. Safety, tolerance and pharmacokinetics of a humanized monoclonal antibody to respiratory syncytial virus in premature infants and infants with bronchopulmonary dysplasia; MEDI-493 Study Group. *Pediatr. Infect. Dis. J.* 17: 110–115.
24. Maloney, D. G., A. J. Grillo-López, C. A. White, D. Bodkin, R. J. Schilder, J. A. Neidhart, N. Janakiraman, K. A. Foon, T. M. Liles, B. K. Dallaire, et al. 1997. IDEC-C2B8 (Rituximab) anti-CD20 monoclonal antibody therapy in patients with relapsed low-grade non-Hodgkin's lymphoma. *Blood* 90: 2188–2195.
25. Tokuda, Y., T. Watanabe, Y. Omuro, M. Ando, N. Katsumata, A. Okumura, M. Ohta, H. Fujii, Y. Sasaki, T. Niwa, and T. Tajima. 1999. Dose escalation and pharmacokinetic study of a humanized anti-HER2 monoclonal antibody in patients with HER2/neu-overexpressing metastatic breast cancer. *Br. J. Cancer* 81: 1419–1425.
26. van de Winkel, J. G., and C. L. Anderson. 1991. Biology of human immunoglobulin G Fc receptors. *J. Leukoc. Biol.* 49: 511–524.
27. Wenig, K., L. Chatwell, U. von Pawel-Rammingen, L. Björck, R. Huber, and P. Sondermann. 2004. Structure of the streptococcal endopeptidase IdeS, a cysteine proteinase with strict specificity for IgG. *Proc. Natl. Acad. Sci. USA* 101: 17371–17376.
28. Davis, P. M., R. Abraham, L. Xu, S. G. Nadler, and S. J. Suchard. 2007. Abatacept binds to the Fc receptor CD64 but does not mediate complement-dependent cytotoxicity or antibody-dependent cellular cytotoxicity. *J. Rheumatol.* 34: 2204–2210.
29. Presta, L. G. 2008. Molecular engineering and design of therapeutic antibodies. *Curr. Opin. Immunol.* 20: 460–470.
30. Scallon, B., A. Cai, N. Solowski, A. Rosenberg, X. Y. Song, D. Shealy, and C. Wagner. 2002. Binding and functional comparisons of two types of tumor necrosis factor antagonists. *J. Pharmacol. Exp. Ther.* 301: 418–426.
31. Martin, W. L., and P. J. Bjorkman. 1999. Characterization of the 2:1 complex between the class I MHC-related Fc receptor and its Fc ligand in solution. *Biochemistry* 38: 12639–12647.
32. Gurbaxani, B. M., and S. L. Morrison. 2006. Development of new models for the analysis of Fc-FcRn interactions. *Mol. Immunol.* 43: 1379–1389.
33. Martin, W. L., A. P. West, Jr., L. Gan, and P. J. Bjorkman. 2001. Crystal structure at 2.8 A of an FcRn/heterodimeric Fc complex: mechanism of pH-dependent binding. *Mol. Cell* 7: 867–877.
34. Osborne, R. 2009. Fresh from the biologic pipeline. *Nat. Biotechnol.* 27: 222–225.
35. Cines, D. B., U. Yasothan, and P. Kirkpatrick. 2008. Romiplostim. *Nat. Rev. Drug Discov.* 7: 887–888.
36. Pan, H., K. Chen, L. Chu, F. Kinderman, I. Apostol, and G. Huang. 2009. Methionine oxidation in human IgG2 Fc decreases binding affinities to protein A and FcRn. *Protein Sci.* 18: 424–433.
37. Chaudhury, C., S. Mehnaz, J. M. Robinson, W. L. Hayton, D. K. Pearl, D. C. Roopenian, and C. L. Anderson. 2003. The major histocompatibility complex-related Fc receptor for IgG (FcRn) binds albumin and prolongs its lifespan. *J. Exp. Med.* 197: 315–322.
38. Chaudhury, C., C. L. Brooks, D. C. Carter, J. M. Robinson, and C. L. Anderson. 2006. Albumin binding to FcRn: distinct from the FcRn-IgG interaction. *Biochemistry* 45: 4983–4990.
39. Steinhauser, I., B. Spänkuch, K. Strebhardt, and K. Langer. 2006. Trastuzumab-modified nanoparticles: optimisation of preparation and uptake in cancer cells. *Biomaterials* 27: 4975–4983.
40. Wuang, S. C., K. G. Neoh, E. T. Kang, D. W. Pack, and D. E. Leckband. 2008. HER-2-mediated endocytosis of magnetic nanospheres and the implications in cell targeting and particle magnetization. *Biomaterials* 29: 2270–2279.
41. Tabrizi, M. A., C. M. Tseng, and L. K. Roskos. 2006. Elimination mechanisms of therapeutic monoclonal antibodies. *Drug Discov. Today* 11: 81–88.
42. Kuester, K., and C. Kloft. 2006. Pharmacokinetics of monoclonal antibodies. In *Pharmacokinetics and Pharmacodynamics of Biotech Drugs*. B. Meibohm, ed. Wiley-VCH Verlag, Weinheim, Germany, p. 45–91.

Division of Drugs, National Institute of Health Sciences, Japan

Ammonium ion level in serum affects doxorubicin release from liposomes

H. SHIBATA, H. SAITO, C. YOMOTA, T. KAWANISHI

Received July 30, 2009, accepted September 14, 2009

Hiroko Shibata, Ph.D., National Institute of Health Science, Kamiyoga 1-18-1, Setagaya-ku, Tokyo 158-8501, Japan
h-shibata@nihs.go.jp

Pharmazie 65: 251–253 (2010) *doi: 10.1691/ph.2010.9255*

In this study, we measured the release of drug from liposome-encapsulated doxorubicin (DXR) in human and mouse serum. While human serum did not induce DXR-release, mouse serum significantly induced DXR-release in a temperature- and time-dependent manner. Release of DXR was clearly observed in ultrafiltrated mouse serum, indicating that low-molecular substances affect DXR-release. Therefore, the level of Na^+, Cl^-, NH_4^+, and urea nitrogen in each type of serum was measured. Only the concentration of NH_4^+ in mouse serum was significantly higher than that in human serum. Furthermore, addition of ammonium acetate to human serum induced DXR release at the same level observed in mouse serum. These results indicate that the NH_4^+ concentration in serum might greatly affect the release of DXR from liposomes.

1. Introduction

Recently, various liposomal products have been developed and applied to clinical treatment (Coukell and Brogden 1998; Maurer et al. 2001). It is a global requirement that evaluation standards for liposomal products are established to ensure their quality (Burgess et al. 2002). The main purpose of using liposomalization is to stabilize drugs *in vivo* and to control release. For example, the serum half-life of DOXIL®, which is the antitumor agent doxorubicin (DXR) encapsulated in a PEGylated or so-called 'stealth' liposome, is about 90 h (Fujisaka et al. 2006), while that of injected DXR is less than 1 h (Mross et al. 1988). Therefore, drug release (or leakage) is one of the most important formulation properties of liposomal products for quality assessment. *In vitro* drug-release tests for appropriately measuring drug release from liposomes would be very useful for assessing lot-to-lot variability or the release characteristics of liposome products. At present, however, few studies have examined how we should assess *in vitro* drug-release appropriately. From this standpoint, we have studied whether or not an *in vitro* release test, which is related to *in vivo* stability, can be established. It's preferable that such an in vitro drug-release test is based on the *in vivo* release mechanism and correlates with the *in vivo* release profiles. In order to achieve *in vivo* relevance, drug release should be measured under conditions that are as near as possible to the physiological condition. Thus, as a first step, we have investigated the utility of human or mouse serum in the assessment of DXR release from stealth liposome-encapsulated DXR (DXR-SL).

2. Investigations, results and discussion

DXR-SL were incubated with mouse or human serum at various temperatures (37, 45, or 52 °C), and the ratio of DXR release was measured. As a result, mouse serum induced significant DXR release from DXR-SL in a temperature- and time-dependent manner (Fig. 1). In the case of human serum, however, the DXR-release rate was extremely low, even at 52 °C. To our knowledge, it has not been reported that drug release from liposomes differs greatly between human serum and mouse serum.

To elucidate this difference, DXR release from DXR-SL was measured in the filtrate of each serum after ultrafiltration (3 kDa or 10 kDa cut-off). Ultrafiltrated mouse serum induced significant DXR release, although it was slightly lower than that in unfiltered serum (Fig. 2A). In human serum, the DXR-release rate in the filtrate was also slightly lower than that in unfiltered serum. This result indicates that low molecular substances largely affect the release of DXR induced in mouse serum. When DXR-SL was incubated with rat or bovine serum, in addition to human and mouse serum, only mouse serum induced DXR release from DXR-SL (Fig. 2B). Next, we compared the DXR-release rate in four kinds of serum: two kinds of fresh serum collected from CD-1 mice and BALB/c mice (prepared in our laboratory), commercial mouse serum that had been used in the above tests, and human serum. As a result, significant DXR release was observed in only the commercial mouse serum, while the DXR-release rate in fresh mouse serum was equivalent to that in human serum (Fig. 2C). These results indicate the possibility that the low molecular substances affecting drug release are specific to the commercial mouse serum.

Therefore, we measured the concentration of typical low molecular substances in blood, such as Na^+, Cl^-, NH_4^+ and urea nitrogen, in each type of serum. Surprisingly, the NH_4^+ level of the commercial mouse serum was 100-fold higher than that of human serum (Fig. 3A). Likewise, the NH_4^+ level was significantly high in another commercially available mouse serum. On the other hand, the concentration of urea nitrogen in the commercial mouse serum was one-twentieth of that in human serum. The concentration of sodium or chloride was normal in all serum. Next, we examined the effect of NH_4^+ level on DXR release from DXR-SL. It was expected that the pH of the commercial mouse serum would be higher than that of human serum. However, there were no differences in pH between mouse and human serum (data not shown). Thus, we added ammonium

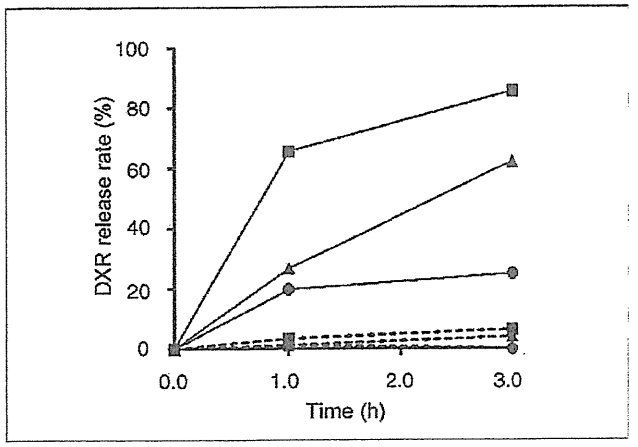

Fig. 1: DXR-release rate in mouse or human serum. DXR-SL (DXR 200 µg/ml) was incubated in human (dashed line) or mouse (solid line) serum (final 90% (v/v)) at 37 °C (circle), 45 °C (triangle), or 52 °C (square) for indicated time

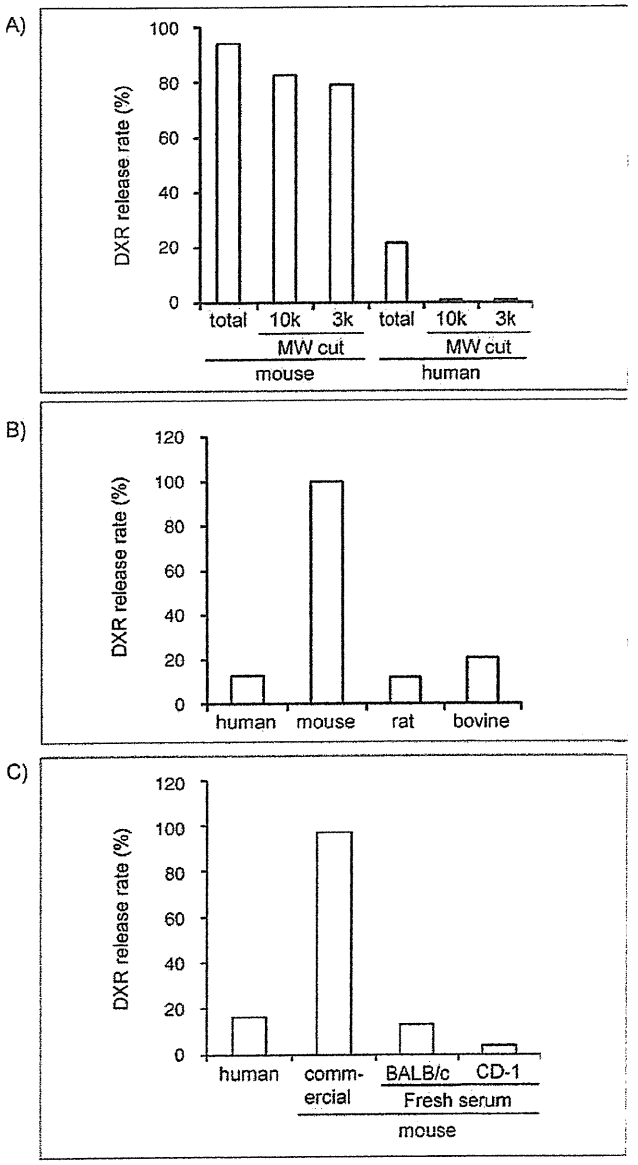

Fig. 2: Effect of difference in serum on DXR-release. A) Effect of ultrafiltrated serum on the DXR-release rate. DXR-SL (DXR 200 µg/ml) was incubated in the filtrate (final 90% (v/v)) for 3 h at 52 °C. DXR-release rate in rat and bovine serum B). and fresh mouse serum collected from BALB/c and CD-1 mice C), in addition to human and mouse serum, were measured after incubation for 3h at 52 °C

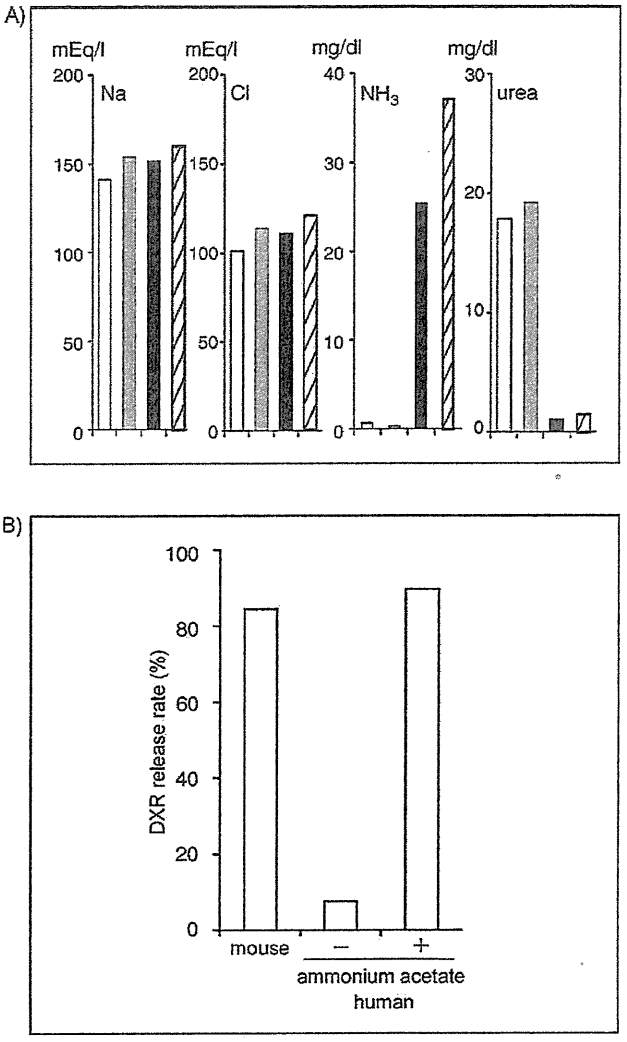

Fig. 3: NH_4^+ level affects DXR release. A) Na^+, Cl^-, NH_4^+ and urea nitrogen in human (white column), fresh mouse serum (gray column), commercial mouse serum (black and shaded column) were measured. B) Ammonium acetate was added to human serum at a final concentration of 1.34 mg/ml which is almost same as the NH_4^+ level in mouse serum. The DXR-release rate in this modified human serum was measured as described in Fig. 1

acetate solution to human serum to the same NH_4^+ level in commercial mouse serum without changing the pH, and measured the DXR-release rate in the adjusted human serum. As in mouse serum, significant DXR release was observed in human serum with ammonium acetate (Fig. 3B). These results suggest that the high NH_4^+ level is one of the causes of the high DXR-release rate in commercial mouse serum.

It is unclear why the NH_4^+ level is markedly increased in commercial mouse serum. Commonly, the blood NH_4^+ level should be measured immediately after blood drawing and centrifugation. Hemolysis and leaving the samples as whole blood at room temperature are causes for elevated test values (Howanitz et al. 1984; Lindner and Bauer 1993). AMP deaminase in red blood cells catalyzes the production of ammonia from protein and amino acids (Nathans et al. 1978). Although we did not investigate the effects in full, we found that, even in human serum, repeating freeze-thaw cycles and long storage tended to increase the DXR-release rate (data not shown). Thus, the high NH_4^+ may be due to a delay in collecting serum after blood drawing, hemolysis, repeating freeze-thaw cycles, or long storage. It is important to stress, however, that the commercial mouse serum used in our examinations is fully compatible with immune assays, such as ELISA or immunostaining, for which it is generally used.

DXR is encapsulated in liposomes by a remote loading method based on the gradient of ammonium sulfate. The mechanism of accumulation is believed to be as follows (Haran et al. 1993). Removal of ammonium sulfate from the extraliposomal medium of liposomes creates an ammonium sulfate gradient $[(NH_4)_2SO_4]_{lip.} > [(NH_4)_2SO_4]_{med.}$ The very high permeability coefficient of neutral NH_3 leads to fast diffusion of NH_3 into the extraliposomal medium. For every NH_3 molecule that leaves the liposome, one proton is left behind, forming a pH gradient across the liposomal membrane. Because DXR is a weakly basic compound (pKa = 8.25), nonionic DXR in the extraliposomal medium diffuses through the lipid bilayer, is protonated and trapped as an ionic form, and accumulates in the intraliposomal aqueous phase by forming a precipitate with sulfate ions. The process can be summarized as an exchange between NH_3 efflux and DXR influx. Therefore, the addition of high concentration ammonium salt to the extraliposomal phase of DXR-SL may induce NH_3 influx into intraliposomes. As a result, the intraliposomal pH may be elevated, and nonionic DXR may diffuse out through the lipid bilayer of liposomes. While the details of the mechanism remain to be elucidated, we speculate that the significant DXR release from DXR-SL in the commercial mouse serum could be caused by high NH_4^+ levels in this way.

Our data revealed that 1) there was almost no DXR release from DXR-SL in human serum, while mouse serum induced significant DXR release; 2) the high NH_4^+ level in mouse serum, especially in commercial mouse serum, is one of the factors leading to the markedly high DXR-release rate; and 3) the concentration of NH_4^+ in the test solution can greatly affect the release of DXR from DXR-SL. Thus, if serum or plasma is used for an *in vitro* drug-release test of liposomal products that are prepared by ammonium sulfate gradient, it will be necessary to control both the lot and the storage period.

3. Experimental

3.1. Materials

Hydrogenated soy phosphatidylcholine (HSPC) and (N-(carbonyl-methoxy polyethyleneglycol 2000)-1,2-distearoyl-sn-glycero-3-phosphoethanolamine (DSPE-PEG2000) were purchased from Nippon Oil and Fat (Tokyo, Japan). Cholesterol (Chol) was of analytical grade (Wako Pure Chemical, Osaka, Japan). Adriacin® injection 10 (Kyowa Hakko Kirin Co., Ltd.), which is doxorubicin (DXR) injection, was purchased from a general sales agency for drugs in Japan. Mouse, rat serum (Valley Biomedical, Inc., VA), and human serum (Biopredic International, Rennes, France) were obtained from KAC Co., Ltd. (Kyoto, Japan). Another mouse serum was obtained from Cedarlane Laboratories Limited (Ontario, Canada). Bovine serum was purchased from Invitrogen (Carlsbad, CA). Fresh mouse serum collected from CD-1 mice was supplied by Charles River (Kanagawa, Japan). Sepharose CL-4B and Sephadex G-25 prepacked columns, PD-10 Desalting Columns, were purchased from GE Healthcare Japan (Tokyo, Japan).

3.2. Liposome preparation

DXR-SL composed of HSPC/Chol/DSPE-PEG2000 (56.5/38/5.4 molar ratio) was prepared by a modified ethanol injection method (Maitani et al. 2001). DXR was encapsulated into liposomes by remote loading using an ammonium sulfate gradient (Lasic et al. 1992). Briefly, all lipids were dissolved in about 5 ml of ethanol, and the ethanol was removed with a rotary evaporator leaving behind about 1 ml of the ethanol solution. Next, 4 ml of 300 mM ammonium sulfate was added to the ethanol solution. Liposomes formed spontaneously after further evaporation of the residual ethanol. After five freeze-thaw cycles, liposomes were extruded through a series of polycarbonate filters (Nucleopore, CA) with pore sizes ranging from 0.4 to 0.1 μm. The mean diameter of resulting liposomes was determined by dynamic light scattering using a DLS-7000 (Otsuka Electronics Co. Ltd., Osaka, Japan). The diameter of extruded liposomes was in the range of 110 ± 30 nm. Following extrusion, liposomes were ultracentrifuged at 80.000 rpm for 45 min at 4 °C, and suspended in normal saline. The concentration of phospholipid was determined by colorimetric assay using Phopholipids C (Wako Pure Chemical Industries, Ltd., Osaka, Japan). DXR was added to the liposomes at a DXR/liposome ratio of 0.2:1 (w/w), and liposomes were incubated for 1 h at 55 °C. The liposome-encapsulated DXR, DXR-SL, was exchanged by eluting through a PD-10 Desalting Column equilibrated with normal saline.

3.3. Release of doxorubicin

DXR-SL (DXR 200 μg/ml) was incubated in each serum (final 90% (v/v)) for indicated time at 37, 45 or 52 °C. After incubation, samples were passed through a Sepharose CL-4B column equilibrated with normal saline to separate the liposomal DXR from serum protein and free drug. The fraction of liposomal DXR was mixed with an equal volume of hydrochloric acid/isopropanol, and the fluorescent intensity was read at 590 nm (excitation 470 nm). The release rate was calculated from the amount of liposomal-DXR. For ultrafiltration, 4 ml of each serum was ultrafiltrated on centrifugal filter units (NMWL 10k or 3k, AmiconUltra, Millipore Corporate Headquarters, Billerica, MA), and 2 ml filtrate was used for release assay. Ammonium acetate was dissolved in water (134 mg/mL) and added to human serum at a final concentration of 1.34 mg/mL which is almost same as the NH_4^+ level in mouse serum.

3.4. Ion levels in serum

Measurement of Na^+, Cl^-, NH_4^+ and urea nitrogen in each serum was outsourced to the Mitsubishi Chemical Medience Corporation (Tokyo, Japan). Na^+ and Cl^- were measured by electrode method. NH_4^+ and urea nitrogen were measured by indophenol colorimetric method (Fujii-Okuda method) and urease-LEDH method, respectively.

Acknowledgements: We thank Dr. Nakashima, Pharmaceutical R&D Division, Janssen Pharmaceutical K.K., for providing critical comments. We also thank Professor Maitani, Hoshi University, Professor Mruyama and Dr. Suzuki, Teikyo University, for advices regarding the preparation of stealth liposome. The present study was supported by the Japan Health Sciences Foundation (KHB1006).

References

Burgess DJ, Hussain AS, Ingallinera TS, Chen ML (2002) Assuring quality and performance of sustained and controlled release parenterals: AAPS workshop report, co-sponsored by FDA and USP. Pharm Res 19: 1761–1768.

Coukell AJ, Brogden RN (1998) Liposomal amphotericin B. Therapeutic use in the management of fungal infections and visceral leishmaniasis. Drugs 55: 585–612.

Fujisaka Y, Horiike A, Shimizu T, Yamamoto N, Yamada Y, Tamura T (2006) Phase 1 clinical study of pegylated liposomal doxorubicin (JNS002) in Japanese patients with solid tumors. Jpn J Clin Oncol 36: 768–774.

Haran G, Cohen R, Bar LK, Barenholz Y (1993) Transmembrane ammonium sulfate gradients in liposomes produce efficient and stable entrapment of amphipathic weak bases. Biochim Biophys Acta 1151: 201–215.

Howanitz JH, Howanitz PJ, Skrodzki CA, Iwanski JA (1984) Influences of specimen processing and storage conditions on results for plasma ammonia. Clin Chem 30: 906–908.

Lasic DD, Frederik PM, Stuart MC, Barenholz Y, McIntosh TJ (1992) Gelation of liposome interior. A novel method for drug encapsulation. FEBS Lett 312: 255–258.

Lindner A, Bauer S (1993) Effect of temperature, duration of storage and sampling procedure on ammonia concentration in equine blood plasma. Eur J Clin Chem Clin Biochem 31: 473–476.

Maitani Y, Soeda H, Junping W, Takayama K (2001) Modified ethanol injection method for liposomes containing beta-sitosterol beta-d-glucoside. J Liposome Res 11: 115–125.

Maurer N, Fenske DB, Cullis PR (2001) Developments in liposomal drug delivery systems. Expert Opin Biol Ther 1: 923–947.

Mross K, Maessen P, van der Vijgh WJ, Gall H, Boven E, Pinedo HM (1988) Pharmacokinetics and metabolism of epidoxorubicin and doxorubicin in humans. J Clin Oncol 6: 517–526.

Nathans GR, Chang D, Deuel TF (1978) AMP deaminase from human erythrocytes. Methods Enzymol 51: 497–502.

J. Sep. Sci. 2011, 34, 2861–2865

Kumiko Sakai-Kato[1]
Shigenori Ota[2]
Kenji Hyodo[3]
Hiroshi Ishihara[3]
Hiroshi Kikuchi[3]
Toru Kawanishi[1]

[1]Division of Drugs, National Institute of Health Sciences, Setagaya-ku, Tokyo, Japan
[2]R&D Department, GL Sciences Inc., Iruma, Saitama, Japan
[3]DDS Research, Formulation Research Laboratories, Pharmaceutical Science and Technology Unit, Eisai Co. Ltd., Tsukuba-shi, Ibaraki, Japan

Received May 13, 2011
Revised June 13, 2011
Accepted June 14, 2011

Short Communication

Size separation and size determination of liposomes

We developed a method for separating liposomes by size and determining their average diameters. Liposomes with different average diameters were separated on a monolithic silica capillary column, and the size of the liposomes corresponding to each peak was determined online with a dynamic light scattering detector coupled to the capillary liquid chromatography system. The calculated diameters for the separated liposomes were similar to the diameter values measured in batch mode. We demonstrate that this combination of a monolithic capillary column and light scattering detection could be used for size separation of liposomes and could provide more details about average diameters than batch-mode analysis.

Keywords: Capillary liquid chromatography / Light scattering detection / Liposomes / Monolithic column
DOI 10.1002/jssc.201100417

1 Introduction

Advances in nanotechnology have contributed to the development of modern drug carrier systems, such as liposomes [1] and polymeric micelles [2, 3], that play an important role in the controlled delivery of pharmacological agents to their targets at a therapeutically optimal rate and dose [4]. Exact knowledge of the sizes of these nanoparticles is essential because size can substantially affect physicochemical and biopharmaceutical behavior. For example, variations in particle size can affect drug release kinetics, transport across biological barriers, and pharmacokinetics in the human body [5–7].

Among the methods for the characterization of macromolecules, flow-assisted techniques, such as size-exclusion chromatography (SEC) [8, 9], hydrodynamic chromatography [10, 11], field-flow fractionation [12–14], and capillary hydrodynamic fractionation [15],] are suitable for separation on the basis of differences in the physical size indexes of the analytes. Electrophoretic separation methods are also used for separation and characterization of colloids that are charged in buffered aqueous solutions [16–18].

SEC is the most commonly used fractionation method for particle sizing. Usually, SEC is performed on a column packed with polymer gel or porous silica microparticles with various pore-size distributions. Polymer samples are separated with such packed SEC columns [8], and nanoparticulate drug carriers, such as liposomes, are often separated from small solutes by means of SEC [19].

Recently, macromolecules, such as a polystyrene polymer, were separated on monolithic silica columns by SEC [20]. Monolithic columns have received much attention as a new technology for HPLC and capillary electrochromatography [21, 22]. These columns consist of a single piece of porous material (most often polymer- or silica-based) with a bimodal pore structure consisting of through-pores (pore size ~1.5–5 m) and mesopores in the skeleton (~10–25 nm) [23]. Because of the high porosity of the monolithic columns, they can be lengthened, thus leading to high separation efficiency.

Although the elution profile obtained by means of SEC provides insight into size distribution, it does not give information about absolute particle size. Dynamic light scattering (DLS), also known as photon correlation spectroscopy, is a non-invasive technique for measuring the size of molecules and particles, typically in the submicron region; and with the latest technology, particles sizes of <1 nm have been measured. DLS is routinely used for size and polydispersity measurements, along with aggregate quantification.

In this report, we describe a system that combines the high resolution of capillary LC with acquisition of absolute diameter data by means of DLS for the online size separation and size determination of liposomal formulations. Although a system using conventional LC coupled with DLS has already been reported [24], ours is the first system that uses capillary LC coupled with DLS.

2 Materials and methods

2.1 Liposome preparation

Liposome samples were prepared by an extrusion procedure. A lipid film containing dipalmitoylphosphatidylcholine,

Correspondence: Dr. Kumiko Sakai-Kato, Division of Drugs, National Institute of Health Sciences, 1-18-1 Kamiyoga, Setagaya-ku, Tokyo 158-8501, Japan
E-mail: kumikato@nihs.go.jp
Fax: +81-3-3700-9662

Abbreviations: DLS, dynamic light scattering; **SEC**, size-exclusion chromatography

cholesterol, and dipalmitoylphosphatidylglycerol (30:40:30, lipid content 20 mM) was suspended in 9.5% sucrose. The suspension was extruded through 200-, 100-, 80-, and 50-nm polycarbonate membranes in that order. Extrusions at every pore size were repeated. Extruded liposome samples were stored in the refrigerator. Samples were dissolved or dispersed in eluent and filtered through a 0.20-μm filter (Millex-LG, Millipore, Tokyo, Japan) prior to being applied to the columns. We used two liposomes with average diameters of 77 and 155 nm, as measured by batch-mode analysis in 10 mM sodium phosphate buffer (pH 7.2) containing methanol (5% v/v), which was also the solvent used as the chromatography eluent.

2.2 LC conditions

The schematics of the analytical system we developed are shown in Fig. 1. Separation was performed with a capillary LC system equipped with a capillary LC micro-flow pump (MP711V; GL Sciences, Tokyo, Japan), a four-port internal sample injector (fixed volume 10 nL; Valco Instrument, Houston, TX, USA), and a capillary ultraviolet–visible (UV–vis) detector (MU701; GL Sciences). Samples were analyzed on a MonoCap Amide column (500 mm × 0.2 mm id; mesopore size ~15 nm or ~20 nm; GL Sciences). The total porosity of the column was estimated using void times of hollow capillary column and monolithic capillary column, and total volume of the column. The eluent was 10 mM sodium phosphate buffer (pH 7.2) containing methanol (5% v/v). The eluent was delivered at a flow rate of 0.1 μL/min, and the column was kept at room temperature. The capillary UV–vis detector was operated at a wavelength of 210 nm. A sample volume of 10 nL was injected for each analysis. Downstream of the UV–vis detector, the same eluent was added by means of a semi-micro-flow pump (NanoSpace 3101 SI-2, Shiseido, Tokyo, Japan) through a T-joint to increase the flow rate. At the increased flow rate, the eluate from the UV–vis detector continuously flowed into the flow cell of a DLS detector via a reducing joint (2 mm, 1/16 inch, GL Sciences). Zetasizer Software was used to calculate the average diameters of the liposomes. A real-time parameter reading from the external device (the UV–vis detector in this case) can be also directly introduced into the optics unit and added to the light scattering sample record.

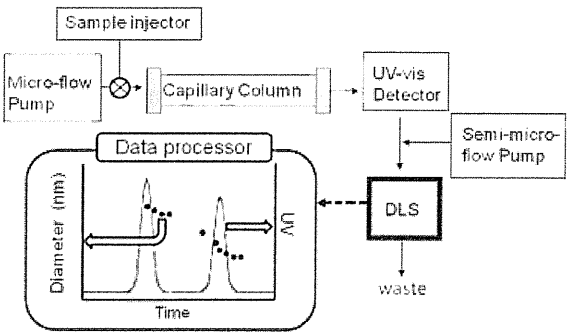

Figure 1. Schematic of analytical system for size separation of liposomes and determination of their average diameters. Samples were injected onto a monolithic capillary column and detected by a microLC UV–vis detector. The flow rate was increased downstream of the detector by means of a semi-micro-flow pump. At the increased rate, the eluate from the UV detector flowed continuously into the DLS detector.

3 Results and discussion

3.1 Separation of liposomes on the monolithic capillary column

In this report, we used the monolithic column which consisted of silica derivatized with an amide group, a neutral hydrophilic group that prohibits adsorption of the samples on the silica monolith by ion-exchange interactions and that permits the analysis of charged soft nanocarriers, such as liposomes derived from biomaterials. As the eluent, 10 mM sodium phosphate buffer (pH 7.2) containing methanol (5% v/v) was used. We attempted to separate liposomes with two different average diameters on a monolithic column with mesopore size of ~15 nm. However, this column did not effectively separate the liposomes (Fig. 2A). When we used a monolithic column with larger mesopores (average size ~20 nm), the resolution was improved (Fig. 2B). Because total porosity is also

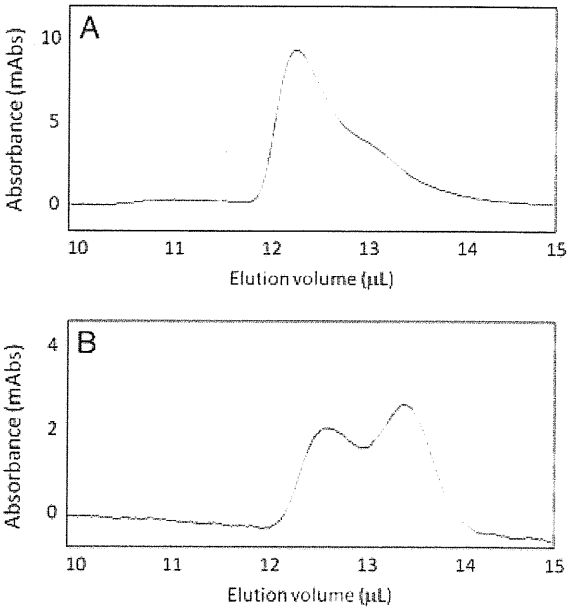

Figure 2. Effect of mesopore size on the separation of liposomes on monolithic columns with (A) ~15-nm mesopores and (B) ~20-nm mesopores. Column: capillary EX nano MonoCap Amide (500 mm × 0.2 mm id); eluent: 10 mM phosphate buffer (pH 7.2) containing 5% methanol; sample: mixture of liposomes with diameters of 155 and 77 nm, as determined by batch measurement; flow rate: 0.1 μL/min; detection wavelength: 210 nm.

increased from 88 to 95%, it is presumed that an increase in throughpore volumes also contributed to the improvement of resolution. SEM images of the latter monolithic column showed the presence of rough surfaces (micron and submicron ranges; Fig. 3). Typically, monolithic columns are more porous than conventional columns packed with spherical particles, and the higher porosity results in much lower column backpressure. Furthermore, the throughpore/skeleton size ratio of 2–4 for the monolithic column was much greater than the 0.25–0.4 ratio typical of columns packed with particles [25]. This higher ratio permits the use of a long column and thus high separation efficiency [26]. Therefore, we connected three 500-mm columns (total length 1500 mm) and then tried the separation again. As expected, the resolution was further improved (Fig. 4A), and the column pressure was only 1.5 MPa. In contrast, the same two liposomes could not be separated by batch-mode DLS analysis (Fig. 4B), and these results show the usefulness of the monolithic column. Also, there is no report that SEC using conventional LC can obtain such a high resolution of liposomes with two different average diameters within 100-nm range. We could not separate liposomes with two different average sizes (111 and 77 nm)

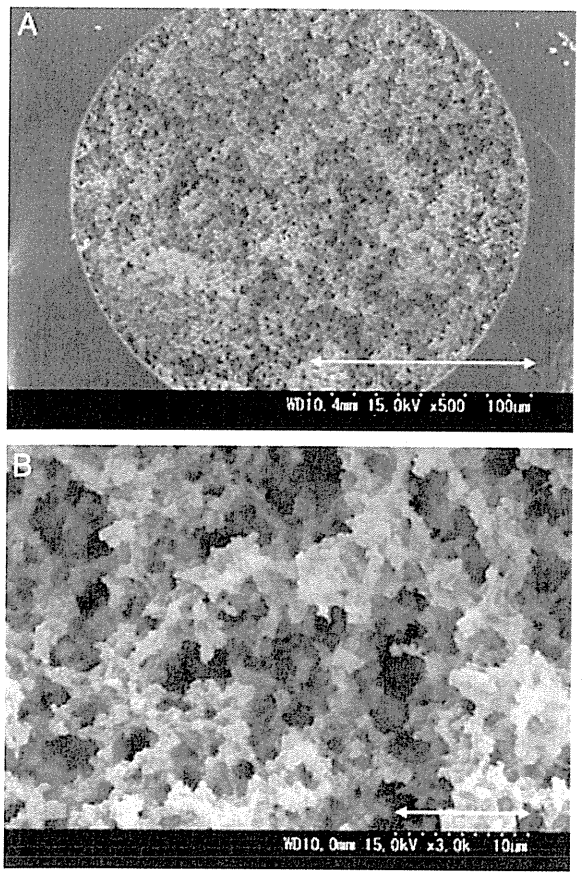

Figure 3. Scanning electron micrographs of monolithic capillary columns. Scale bars correspond to 100 μm for (A) and 10 μm for (B).

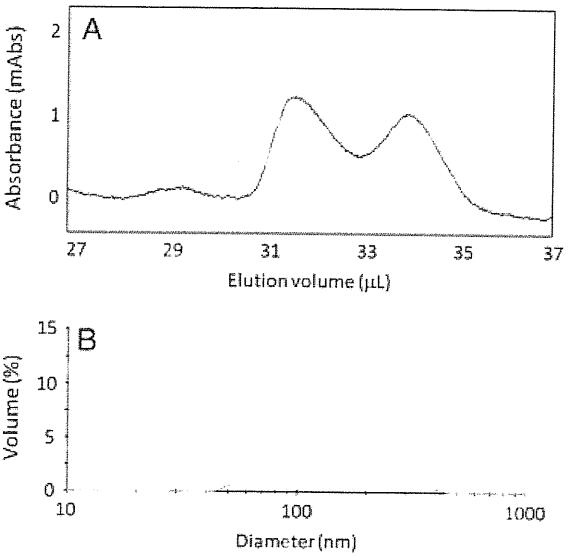

Figure 4. Analysis of liposomes in (A) flow-assisted mode and (B) batch mode. (A) Analysis in flow-assisted mode. Column: capillary EX nano MonoCap Amide (500 mm × 0.2 mm id) ×3; eluent: 10 mM phosphate buffer (pH 7.2) containing 5% methanol; sample: mixture of liposomes with sizes of 155 and 77 nm, as determined by batch measurement; flow rate: 0.1 μL/min; detection wavelength: 210 nm. (B) Analysis in batch mode with DLS detection. Sample: mixture of liposomes with diameters of 161 and 77 nm; dispersant: 10 mM phosphate buffer (pH 7.2) containing 5% methanol.

(data not shown). Therefore, the separation of 80 nm size difference is possible by this system.

3.2 Online data acquisition by DLS

Next, we evaluated a system that combined capillary LC with DLS detection. The DLS data were accumulated continuously and analyzed every 3 s, and the software recorded all correlation functions and intensity values. Because the volume of the DLS flow cell was 135 μL and the detection volume was 5 μL, and the flow rate of the capillary LC system was <1 μL/min, we increased the flow rate downstream of the UV–vis detector by adding the same eluent to the flow by means of a semi-micro-flow pump through a T-joint downstream of the detector. However, the flow was diluted by the additional eluent. Therefore, we examined the effect of the increased flow rate on the intensity of scattered light to make sure that DLS detection was still feasible at the higher flow rate. At flow rates ranging from 50 to 10 μL/min, DLS detection was possible, and diameters of the liposomes could be calculated. Figure 5A shows the average diameter and external UV input for monodisperse liposomes injected onto the monolithic column. The system was operated at a flow rate of 50 μL/min. From the single peak that was detected, we calculated an average diameter of 166 nm, which was close to the expected value (155 nm) for this liposome dispersion, as indicated by batch-mode

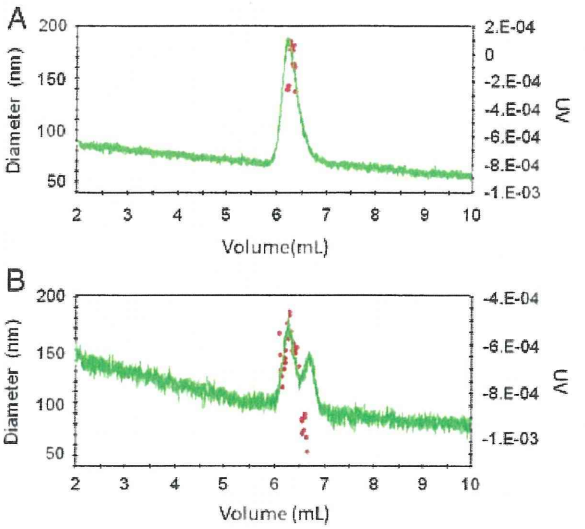

Figure 5. Plots of diameters and UV absorption versus elution volumes for liposomes injected onto a monolithic column. Column: capillary EX nano MonoCap Amide (500 mm × 0.2 mm id); eluent: 10 mM phosphate buffer (pH 7.2) containing 5% methanol; sample: liposomes with diameters of (A) 155 nm and (B) mixture of liposomes with diameters of 155 and 77 nm as determined by batch measurement. Capillary LC flow rate: 0.1 μL/min; semi-micro-flow pump flow rate: 50 μL/min; detection wavelength: 210 nm. AU: arbitrary unit.

analysis. We ascribed the similarity of the values to the low column backpressure, which did not affect the diameter of liposomes. The run-to-run repeatability of the calculated diameter for the eluted sample was determined to be 1.2% (RSD, $N = 3$). As far as I know, there have been no reports that the semi-micro-LC column or conventional column can separate liposomes with two different average diameters within 100-nm range. If we can use semi-micromonolithic LC column or conventional monolithic column long enough to separate liposomes with two different average diameters within 100-nm range, it is not required to dilute eluate from column before detector.

Next, we used the developed system to analyze a dispersion of liposomes with two different diameter ranges. Figure 5B shows the diameter and external UV input versus elution volumes for liposomes, separated onto a monolithic column. The size separation of the liposomes was good, and average diameters for the two detected peaks were calculated as 164 and 77 nm; these values were also similar to the values measured in batch mode, 155 and 77 nm, respectively.

4 Concluding remarks

We developed a system for simultaneous size separation and size determination of liposomes using a capillary LC system with DLS detection. By changing the mesopore size, we could improve the separation of liposomes with different average diameters. Because the column had a low backpressure, resolution could easily be increased by lengthening the column. After increasing the flow rate with a second pump, we used DLS detection to determine the diameters of the separated liposomes. Analysis with this system provided more-detailed information than conventional batch-mode analysis about the size of the liposomes, which affects their physicochemical and biopharmaceutical behavior.

The authors are grateful for financial support from the Research on Publicly Essential Drugs and Medical Devices Project (The Japan Health Sciences Foundation), a Health Labor Sciences Research Grant from the Ministry of Health, Labor and Welfare (MHLW), and KAKENHI (21790046) from the Ministry of Education, Culture, Sports, Science, and Technology (MEXT), Japan.

The authors have declared no conflict of interest.

5 References

[1] Bangham, A. D., Standish, M. M., Watkins, J. C., *J. Mol. Biol.* 1965, *13*, 238–252.

[2] Nishiyama, N., Kataoka, K., *Pharmacol. Ther.* 2006, *112*, 630–648.

[3] Torchilin, V. P., Lukyanov, A. N., Gao, Z., Papahadjopoulos-Sternberg, B., *Proc. Natl. Acad. Sci. USA.* 2003, *100*, 6039–6044.

[4] Ferrari, M., *Nat. Rev. Cancer.* 2005, *5*, 161–171.

[5] Hillyer, J. F., Albrecht, R. M., *J. Pharm. Sci.* 2001, *90*, 1927–1936.

[6] Lamprecht, A., Bouligand, Y., Benoit, J. P., *J. Control Release* 2002, *84*, 59–68.

[7] Rejman, J., Oberle, V., Zuhorn, I. S., Hoekstra, D., *Biochem. J.* 2004, *377*, 159–169.

[8] Kirkland, J. J., *J. Chromatogr. A.* 1976, *125*, 231–250.

[9] Huang, S. S., in: Wu, C.-S. (Eds.), *Handbook of Size Exclusion Chromatography and Related Techniques*, Marcel Dekker, New York 2004, p. 677.

[10] Small, H., Colloid, J., *Interface Sci.* 1974, *48*, 147–161.

[11] Williams, A., Varela, E., Meehan, E., Tribe, K., *Int. J. Pharm.* 2002, *242*, 295–299.

[12] Giddings, J. C., *Science* 1931, *260*, 1456–1465.

[13] Giddings, J. C., *Anal. Chem.* 1995, *67*, 592A–598A.

[14] Moon, M. H., Park, I., Kim, Y., *J. Chromatogr. A* 1998, *813*, 91–100.

[15] Silebi, C. A., Dosramos, J. G., *J. Colloid. Interface Sci.* 1989, *130*, 14–24.

[16] VanOrman, B. B., McIntire, G. L., *J. Microcolumn Sep.* 1989, *1*, 289–293.

[17] Ahmadzadeh, H., Dua, R., Presley, A. D., Arriaga, E. A., *J. Chromatogr. A* 2005, *1064*, 107–114.

[18] Rezenom, Y. H., Wellman, A. D., Tilstra, L., Medley, C. D., Gilman, S. D., *Analyst* 2007, *132*, 1215–1222.

[19] Grabielle-Madelmont, C., Lesieur, S., Ollivon, M., *J. Biochem. Biophys. Methods* 2003,*56*, 189–217.

[20] Ute, K., Yoshida, S., Kitayama, T., Bamba, T., Harada, K., Fukusaki, E., Kobayashi, A., Ishizuka, N., Minakuchi, H., Nakanishi, K., *Polymer J.* 2006, *38*, 1194–1197.

[21] Minakuchi, H., Nakanishi, K., Soga, N., Ishizuka, N., Tanaka, N., *Anal. Chem.* 1996, *68*, 3498–3501.

[22] Peters, E. C., Petro, M., Svec, F., Frechet, J. M. J., *Anal. Chem.* 1998, *70*, 2296–2302.

[23] Tanaka, N., Kobayashi, H., Nakanishi, K., Minakuchi, H., Ishizuka, N., *Anal. Chem.* 2001, *73*, 420A–429A.

[24] Zetasizer nano application note, Absolute size exclusion chromatography, MRK877-01, Marvern. http://www.malvern.com/malvern/kbase.nsf/allbyno/KB001244/$file/MRK877-01.pdf.

[25] Unger, K. K., *Porous Silica (Journal of Chromatography Library–vol. 16)*, Elsevier, Amsterdam 1979.

[26] Miyamoto, K., Hara, T., Kobayashi, H., Morisaka, H., Tokuda, D., Horie, K., Koduki, K., Makino, S., Núñez, O., Yang, C., Kawabe, T., Ikegami, T., Takubo, H., Ishihama, Y., Tanaka, N., *Anal. Chem.* 2008, *80*, 8741–8750.

Stabilization of Liposomes in Frozen Solutions Through Control of Osmotic Flow and Internal Solution Freezing by Trehalose

KEN-ICHI IZUTSU, CHIKAKO YOMOTA, TORU KAWANISHI

National Institute of Health Sciences, Setagaya-ku, Tokyo 158-8501, Japan

Received 22 September 2010; revised 7 December 2010; accepted 25 January 2011

Published online 16 February 2011 in Wiley Online Library (wileyonlinelibrary.com). DOI 10.1002/jps.22518

ABSTRACT: The purpose of this study was to elucidate the effect of trehalose distribution across the membrane on the freeze-related physical changes of liposome suspensions and their functional stability upon freeze–thawing. Cooling thermal analysis of 1,2-dipalmitoyl-*sn*-glycero-3-phosphocholine liposome suspensions showed exotherm peaks of bulk (−15°C to −25°C) and intraliposomal (approx. −45°C) solution freezing initiated by heterogeneous and homogeneous ice nucleation, respectively. The extent of the intraliposomal solution freezing exotherm depended on liposome size, lipid composition, cosolutes, and thermal history, suggesting that osmotic dehydration occurred due to the increasing difference in solute concentrations across the membrane. A freeze–thawing study of carboxyfluorescein-encapsulated liposomes suggested that controlling the osmotic properties to avoid the freeze-induced intraliposomal solution loss either by rapid cooling of suspensions containing trehalose in both sides of the membrane (retention of the intraliposomal supercooled solution) or by cooling of suspensions containing trehalose in the extraliposomal media prior to freezing (e.g., osmotic shrinkage) led to higher retention of the water-soluble marker. Evaluation and control of the osmotically mediated freezing behavior by optimizing the formulation and process factors should be relevant to the cryopreservation and freeze-drying of liposomes. © 2011 Wiley-Liss, Inc. and the American Pharmacists Association J Pharm Sci 100:2935–2944, 2011

Keywords: liposomes; formulation; stabilization; thermal analysis; osmosis; calorimetry (DSC); excipients; freeze-drying

INTRODUCTION

The increase in the variety and clinical relevance of liposomal formulations has enhanced the importance of the freezing and freeze-drying processes for the distribution and long-term storage of the drug delivery systems that are not chemically and/or physically stable enough as aqueous suspensions.[1–4] These processes, however, expose the lipid systems to various stresses including ice growth, pH change, concentration of the surrounding solutes, and dehydration that often damage their structural integrity and pharmaceutical functions [e.g., release of active pharmaceutical ingredients (APIs)] of liposomes. Retaining water-soluble APIs is a particular challenge for development of liposome formulations.[1] Formulation and process design that are based on an understanding of the freeze-related stresses and required stabilization mechanisms should improve the stability of various liposome pharmaceuticals.[1–3]

Disaccharides (e.g., trehalose and sucrose) and some amino acids have been applied to protect the lipid systems from chemical and physical changes during freeze–thawing (cryoprotectants) and freeze-drying (lyoprotectants).[1,3] The stabilization of liposomes by disaccharides is explained mainly by three mechanisms. Some saccharides substitute the water molecules necessary to retain the supramolecular phospholipid assembly through molecular interactions with hydrophilic phospholipid head groups (water substitution).[5–7] The saccharides also form highly viscous amorphous freeze-concentrated phases and dried solids that prevent direct contact between liposome vesicles (bulking).[1,8,9] The reduced mobility of the surrounding molecules helps improve the chemical and physical stability of liposomes (vitrification). Use of the stabilizers is mostly dependent on empirical trial and error through analysis of the morphological (e.g., size) and functional (e.g., API or marker

Correspondence to: Ken-ichi Izutsu (Telephone: +81-3-3700-1141; Fax: 81-3-3707-6950; E-mail: izutsu@nihs.go.jp)

Journal of Pharmaceutical Sciences, Vol. 100, 2935–2944 (2011)

retention) traits of the resulting suspensions or dried solids.

Longstanding cryopreservation studies of living cells and microorganisms provide precepts valuable for the protection of liposomes against the freeze-induced stresses.[10–14] The cooling of cell and liposome suspensions induces the freezing of bulk solutions initiated by heterogeneous ice nucleation at the surface of containers or impurities (−5°C to −25°C) and the freezing of spatially restricted internal solutions initiated by homogeneous (spontaneous) ice nucleation (−25°C to −45°C).[15–21] The bulk solution freezing and the accompanying significant concentration of solutes surrounding the living cells and liposomes induce osmotic stress that removes the internal solution before they freeze, leading to morphological changes observable by microscopic methods (e.g., optical microscope and cryo-transmission electron microscopy).[21,22] Because the intracellular ice formation (IIF) is widely recognized to cause lethal damage through disordering of the complex membrane and intracellular structure (e.g., organelle), cryopreservation of the living cells and microorganisms is usually performed in two ways that prevent IIF, namely by slow cooling of suspensions containing extracellular solutes (cell dehydration) and by rapid cooling of the suspensions containing high-concentration membrane-permeating solutes [e.g., dimethyl sulfoxide (DMSO), cytoplasm vitrification].[12] On the contrary, only limited studies have been performed on the stabilization of liposomes taking various freezing-related physical changes into account.[17,23–25]

The purpose of this study was to elucidate the effect of intra- and extraliposomal trehalose on the freeze-related physical changes and functional stability of liposomes during freeze–thawing. The effect of saccharide distribution across the membrane on the stability of liposomes is of particular interest for formulation purposes because the liposome preparation methods significantly affect allocation of the nonpermeating solutes. Different solute concentrations across the membrane induce osmotic flow that shrinks or swells the liposomes in the aqueous suspensions.[4,22,26] Literature claims the requirement of disaccharides on both sides of the membrane to protect liposomes from freezing- and lyophilization-related stresses (e.g., addition before extrusion).[8] Recent reports suggested that the rational setting of different intra- and extraliposomal trehalose concentrations confers better stabilization.[1,27] Effect of trehalose on the freeze-related physical phenomena (e.g., freeze-induced dehydration and intraliposomal solution freezing) and functional stability of liposomes were studied mainly through thermal analysis and through the retention of encapsulated carboxyfluorescein (CF).[27,17]

MATERIALS AND METHODS

Materials

Chemicals obtained from the following sources were used without further purification: 1-palmitoyl-2-oleoyl-*sn*-glycero-3-phosphocholine (POPC), 1,2-dimyristoyl-*sn*-glycero-3-phosphocholine (DMPC), 1,2-dipalmitoyl-*sn*-glycero-3-phosphocholine (DPPC), and 1,2-distearoyl-*sn*-glycero-3-phosphocholine (DSPC) (NOF Co., Tokyo, Japan); trehalose dihydrate, glucose, sucrose, and 5(6)-CF (Sigma–Aldrich Co., St. Louis, Missouri); DMSO, xylitol, and glycerol (Wako Pure Chemical Co., Osaka, Japan); and dextran 4000–6000 (Serva Electrophoresis GmbH, Heidelberg, Germany).

Preparation of Liposome Suspensions

Phospholipid films were obtained by drying their solution in a chloroform and methanol mixture (2:1) under vacuum at temperatures above the main transition temperature (T_m). Liposome suspensions were prepared by using a hand-held extruder (Avanti Polar Lipids, Alabaster, Alabama). The films hydrated by 10 mM Tris–HCl buffer (6%, w/w; pH 7.4) were extruded 12 times through a polycarbonate membrane filter (0.1–0.8 μm pore, 0.2 μm unless otherwise mentioned; Whatman, Maidstone, UK) while maintaining the apparatus at room temperature (POPC) or at temperatures 10 to 15°C higher than the T_m of the respective lipids. The DPPC liposomes extruded through the smaller pore membranes (0.1 and 0.2 μm) were reported to have a unilamellar structure, whereas those extruded through the larger pore membranes (0.4 and 0.8 μm) contained increasing ratios of multilamellar vesicles.[29,30] The term "0.2 μm liposome" will be used in the text given below to denote samples prepared by extrusion through the respective pore size membranes.

Some liposome suspensions containing the excipients predominantly in the extraliposomal media were prepared by adding the excipients approximately 30 min prior to the thermal analysis and freeze–thawing experiments. Those containing excipients in both the inside and outside of the membranes were prepared by the extrusion of lipids hydrated with the excipient-containing solutions. Some suspensions were eluted through Sephadex G-25 desalting columns (PD-10; GE Healthcare Bio-Sciences AB, Uppsala, Sweden) equilibrated with the Tris–HCl buffer to obtain samples containing the excipient mainly in the intraliposomal solutions. The concentrations of DPPC in the column-eluted suspensions were obtained by phosphorous assay.[31] Measurement of the DPPC concentrations in the liposome suspensions indicated that approximately 90% of the liposomes passed through the Sephadex columns.

DOI 10.1002/jps

Thermal Analysis

Thermal analysis of the frozen liposome suspensions was performed by using a differential scanning calorimeter (DSC Q10; TA Instruments, New Castle, Delaware) equipped with a refrigerating system and data processing software (Universal Analysis 2000, TA Instruments). Aliquots [10 μL, 4% (w/w) lipid] of suspensions in hermetic aluminum cells were cooled from 25°C to −70°C at varied speeds (1–10°C/min) and then heated to 25°C at a scanning rate of 5°C/min. The intensity of the intraliposomal solution freezing exotherm was shown as their ratio to the lipid content (J/g lipid). Some DPPC liposome suspensions were heat-treated at 45°C for 3 min before the cooling scan. The cooling scan of some suspensions were paused at certain temperatures (−10°C to −35°C) and maintained those temperatures for 30 or 60 min before further cooling to study the effect of low temperature storage on the physical changes. The column-eluted liposome suspensions were subjected to thermal analysis without the concentration adjustment. The homogeneous ice formation exotherms of these suspensions were calculated using the phosphate concentration data.

Measurement of Liposome Size by Dynamic Light Scattering

The size distribution of liposomes suspended in the Tris–HCl buffer (0.08% DPPC, 25°C) was determined using a dynamic light scattering (DLS) spectrophotometer (Photal DLS-7100SL; Otsuka Electronics Co., Osaka, Japan) with a He–Ne laser (632.8 nm) and a scattering angle (90°; 50 scans).

CF Retention Study

Dried DPPC films were hydrated with solutions containing 25 mM 5(6)-CF, 10 mM Tris–HCl buffer, and 0% or 12% trehalose, adjusted to pH 7.4 by NaOH. The CF-loaded vortexed multilamellar liposome suspensions (6% lipid, w/w) were prepared by extrusion through a 0.2-μm pore filter, and then eluted through the Sephadex G-25 column equilibrated with the buffer or trehalose-containing buffer. Freeze–thawing of the suspension was performed using the DSC system while the thermal profiles were simultaneously monitored. Aliquots of the liposome suspensions (10 μL, 4% DPPC, w/w) in unsealed aluminum pans were cooled to −35°C or −70°C at varied cooling speeds (1–10°C/min), and then heated to 25°C at 10°C/min on the DSC furnace. The freeze–thawed liposome suspensions were diluted by adding the Tris–HCl buffer or trehalose-containing buffer solutions (10 mL) in the glass tubes. The mildly agitated liposome suspensions underwent fluorescence measurement using a spectrometer (FP-6500; JASCO Corp., Tokyo, Japan). After the initial fluorescence measurements of the suspensions (2 mL) at 460 nm (excitation) and 550 nm (emission), those of the membrane-perturbed liposome suspensions were obtained by the addition of aliquots (20 μL) of Triton X-100. The CF leakage ratio was calculated using the following equation:

$$\%\,\text{Leakage} = \frac{\text{Initial fluorescence of treated sample} - \text{initial fluorescence of control}}{(\text{Final fluorescence of treated sample} - \text{initial fluorescence of control})} \times 100$$

RESULTS AND DISCUSSION

Freeze-Induced Changes in Liposome Suspensions

Figure 1 shows a thermogram of a frozen DPPC liposome suspension (4% in 10 mM Tris–HCl buffer, 0.2 μm) cooled at 5°C/min. The suspension showed a large exothermic peak of the freezing of the bulk solution (heterogeneous ice nucleation) at approximately −20°C and a smaller second exothermic peak of the freezing of the intraliposomal solution (homogeneous ice nucleation) at approximately −45°C.[15,17,32] The lower temperature exotherm disappeared by prior addition of a membrane-perturbing surfactant (1% Triton X-100), which supported the aforementioned definition of the peak rather than other interpretations (e.g., freezing of phosphatidylcholine headgroups) of the exotherm (data not shown).[33] The temperature

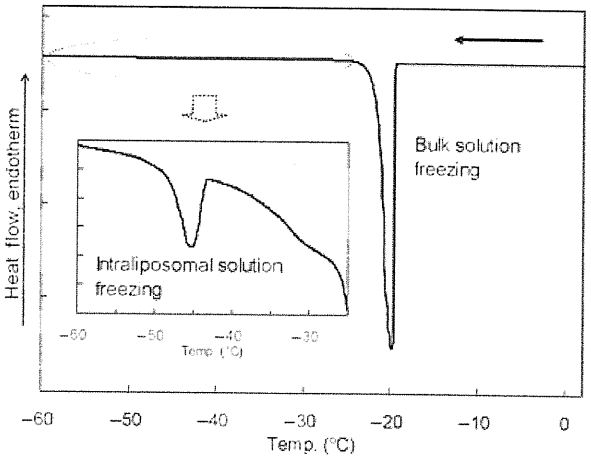

Figure 1. Cooling thermogram of a frozen DPPC liposome suspension. An aliquot (10 μL) of liposome suspension (4% lipid, w/w) in Tris–HCl buffer (10 mM, pH 7.4) was cooled from room temperature to −70°C at 5°C/min.

of the bulk solution freezing peak varied greatly between the scans. Some suspensions also showed a broad exotherm at approximately −30°C. The exotherm suggested the freezing of solutions released from the liposomes (dehydration) and/or freezing of the internal solutions initiated by external ice crystals that penetrated through the membrane.[12,16,34] The varied shape and overlapping of the peak with the large bulk solution freezing exotherm made further characterization difficult in this study. The frozen liposome suspensions showed only a gradual shift of the thermogram before the large ice melting endotherm during their heating scans (data not shown). DLS measurement of the DPPC liposome suspensions indicated a mean diameter of 203.9 ± 10.6 nm before the thermal analysis (three different preparations). Standard deviation of the liposome size obtained in each measurement was within 5% of the average value.

The effects of cooling speeds on the internal solution freezing exotherm of liposomes differing in size and lipid composition are shown in Figure 2. Slower cooling of the DPPC liposome suspension (0.2 μm) reduced the exotherm, indicating loss of the supercooled intraliposomal solution during the scan (Fig. 2a; 1 –2°C/min). The extraliposomal ice growth and concomitant concentration of solutes should generate osmotic forces that induce water evacuation from liposomes. Reported freeze-induced morphological rearrangement into multilamellar liposomes may also reduce the intraliposomal solution content.[4] The width of the bulk solution freezing peak got narrower in the slower cooling, suggesting a certain time required for the ice growth (data not shown). On the contrary, the limited effect of the cooling speed on the peak width of the intraliposomal solution freezing exotherm suggested independent ice formation in the individual liposomes. A certain amount of the intraliposomal solution interacting (hydrating) with the membrane lipid and/or solute molecules should remain unfrozen even below the intraliposomal solution freezing temperature.[11,11]

Reduction of the intraliposomal solution freezing exotherm was more apparent in the DPPC liposome suspensions temporarily (30 min) kept at temperatures between the bulk and the intraliposomal solution freezing during the cooling scan (Fig. 3). The finding that the intraliposomal solution freezing exotherm of a suspension held at −25°C was smaller than those of suspensions held at −30°C or −35°C suggested faster loss of the supercooled solutions in the temperature range just below the bulk solution freezing. Longer exposure to the temperature range should be one of the reasons for the reduction in the exotherms with the slower cooling. On the contrary, holding the suspension at a temperature above the bulk solution freezing temperature showed no apparent effect on the intraliposomal solution freezing

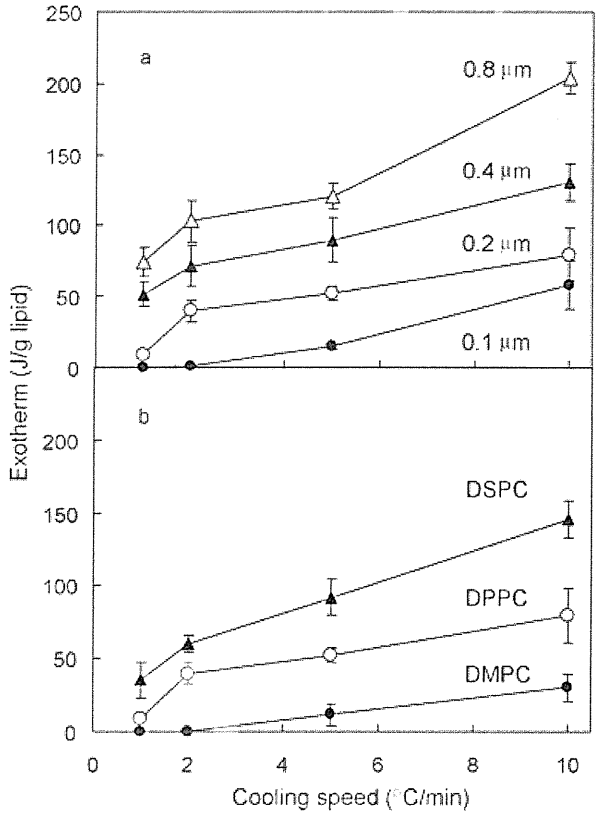

Figure 2. Effects of cooling speed on internal solution freezing exotherm of liposome suspensions with differing (a) extrusion membrane pore sizes (DPPC; 0.1 μm: •, 0.2 μm: ○, 0.4 μm: ▲, and 0.8μm: △) and (b) lipid compositions (0.2 μm; DMPC: •, DPPC: ○, and DSPC: ▲). Aliquots of liposome suspensions (10 μL, 4% lipid in 10 mM Tris–HCl buffer) were cooled at 1–10°C/min (average ± SD, $n = 3$).

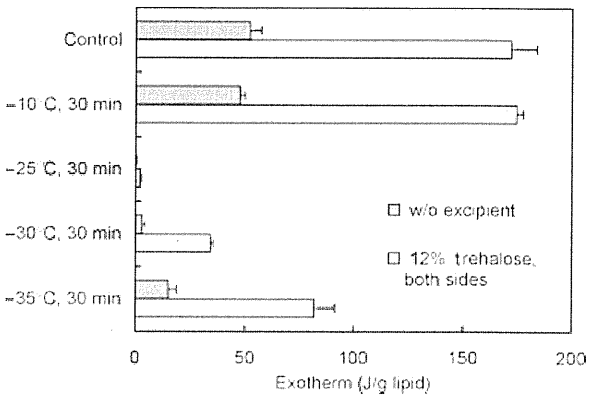

Figure 3. Effect of low temperature holding on internal solution freezing exotherms of DPPC liposome suspensions containing trehalose (0% or 12%, w/w) on both sides of the membrane (10 μL, 4% lipid in Tris–HCl buffer, 0.2 μm). The suspensions were held at different temperatures (−10°C to −35°C) for 30 min during cooling scans at 5°C/min.

DOI 10.1002/jps

exotherm. The absence of apparent osmotic driving force may explain the limited effect of storage at above the bulk solution freezing temperature.

The DPPC liposome suspensions extruded through larger pore size filters (e.g., 0.4 and 0.8 μm) showed larger intraliposomal solution freezing exotherms (Fig. 2a). Factors including the possibility of higher initial solution contents per lipid weight, limited membrane disordering associated with the curvature, and slower dehydration due to the increase in multilamellar membranes would explain the large exotherms. Liposomes composed of phosphatidylcholines of different acyl chain lengths showed retention of the intraliposomal solution down to the homogeneous ice formation temperature in the order of DMPC < DPPC < DSPC (Fig. 2b). The intraliposomal solution freezing exotherm was not observed in the thermal analysis of POPC liposome suspensions (data not shown). All the liposome membranes are below their T_m (POPC: −5°C, DMPC: 24°C, DPPC: 41°C, DSPC: 54°C) at the bulk solution freezing temperature.[35] Possible differences in the membrane fluidity and rigidity would cause the freeze-induced dehydration to vary.

Effect of Trehalose Distribution on Freezing Profiles of Liposome Suspensions

The effects of intra- and extraliposomal trehalose on the freezing behavior of liposome suspensions were studied. The DPPC liposome suspensions containing trehalose on both sides of the membrane showed larger intraliposomal solution peaks that suggest reduced solution loss upon the bulk solution freezing. For example, cooling of the 0.2 μm DPPC suspensions at 10°C/min resulted in exotherms of approximately 80 and 200 J/g lipid, respectively, in the absence and presence of trehalose (Figs. 2 and 4). The addition of trehalose also lowered the peak temperature of the exotherm (approx. 3°C at 12% trehalose, w/w).[18,34] The trehalose-containing liposome lost a larger amount of the internal supercooled solution during the slower cooling of the suspensions. Temporary pausing of the cooling scan suggested a faster loss of the supercooled solution near the bulk solution freezing temperature (−25°C), also in the trehalose-containing liposome suspensions (Fig. 3). The addition of various low-molecular-weight saccharides and polyols to both sides of the lipid membrane increased the freezing exotherm of the intraliposomal solutions, suggesting that slower freeze-induced dehydration occurred due to the colligatively determined osmotic effect (Fig. 5). The limited effect of dextran on the exotherm could be explained by its lower molar concentration and its possible exclusion from the vicinity of the liposomes in the freeze-concentrated non-ice phase.[36] The large (0.4 and 0.8 μm) or lower fluidity (DSPC) liposomes retained higher amounts of

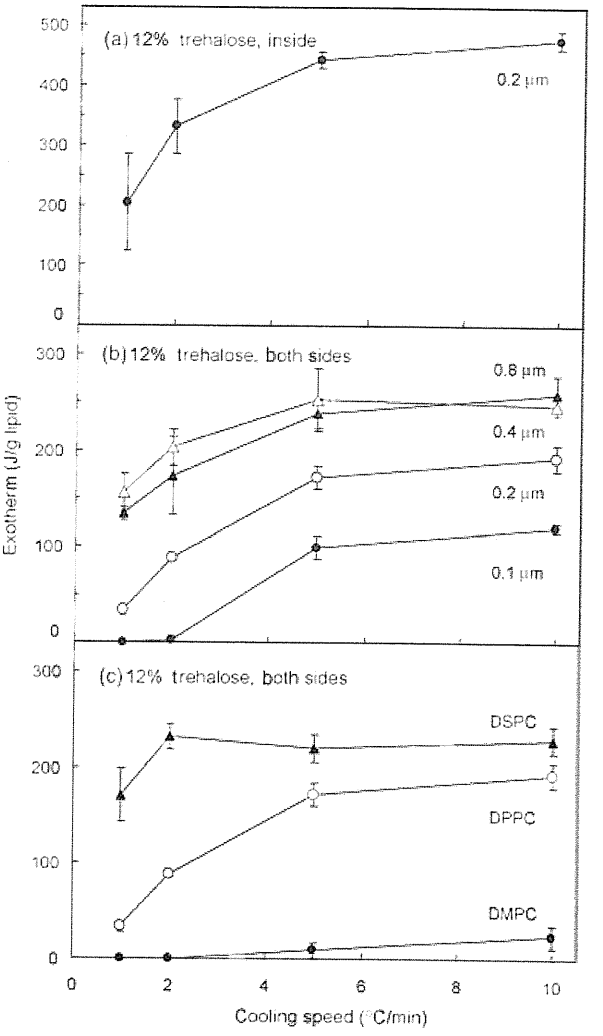

Figure 4. Internal solution freezing exotherms of liposome suspensions containing trehalose (12%, w/w) on (a) the inside and (b, c) both sides of liposomes. Aliquots of suspensions (10 μL, 4% lipid in 10 mM Tris–HCl buffer) containing liposomes with (b) differing extrusion membrane pore sizes (DPPC; 0.1 μm: •, 0.2 μm: ○, 0.4 μm: ▲, and 0.8 μm: △) and (c) lipid compositions (0.2 μm; DMPC: •, DPPC: ○, and DSPC: ▲) were cooled at 1–10°C/min (average ± SD, $n = 3$).

freezable intraliposomal solution in the presence of trehalose on both sides of the membrane (Figs. 4b and 4c).

1,2-Dipalmitoyl-*sn*-glycero-3-phosphocholine liposomes containing trehalose on one side of the membrane showed different freezing behaviors. The addition of higher concentration trehalose to the extraliposomal media reduced the intraliposomal solution freezing exotherm (Fig. 6). The difference in the osmotic pressures across the membrane should induce solution flow that dehydrates the liposomes both prior to cooling and after the bulk solution freezing. The

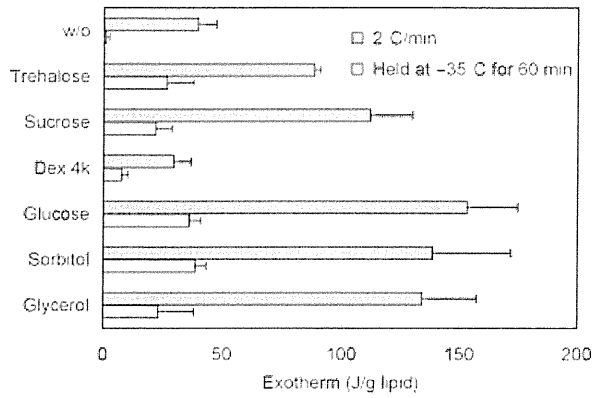

Figure 5. Effect of various extraliposomal solutes (12%, w/w) on internal solution freezing exotherms of DPPC liposome suspensions (10 μL, 4% lipid in 10 mM Tris–HCl buffer, 0.2 μm) obtained via cooling scans at 2°C/min (average ± SD, $n = 3$). Some suspensions were held at −35°C for 60 min during the scan.

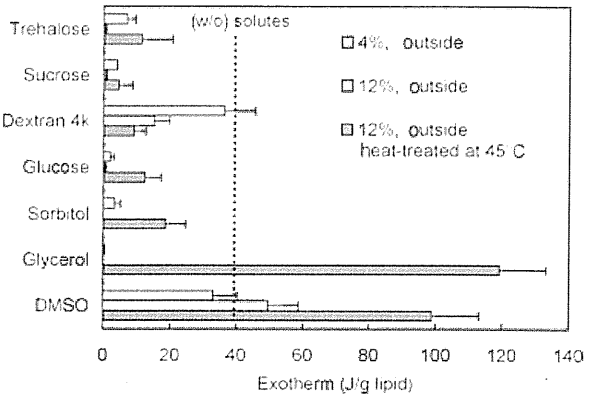

Figure 7. Effect of various extraliposomal solutes (4% and 12%, w/w) on internal solution freezing exotherms of DPPC liposomes obtained via cooling scans of suspensions (10 μL, 4% DPPC in 10 mM Tris–HCl buffer, 0.2 μm) from room temperature to −70°C at 2°C/min. Some suspensions were heat-treated at 45°C for 3 min before the cooling analysis (average ± SD, $n = 3$).

absence of a broad exotherm between the bulk and intraliposomal solution freezing peaks suggested that liposome dehydration before the bulk solution freezing (e.g., osmotic shrinkage) had occurred rather than the freeze-induced dehydration (data not shown).

Other low-molecular-weight saccharides and polyols in the extraliposomal media also reduced the intraliposomal solution freezing exotherms of the DPPC liposomes (Fig. 7). The extraliposomal dextran showed smaller effect to reduce the exotherm compared with the lower-molecular-weight excipients. Prior heat treatment of the liposome suspensions at above T_m of DPPC (45°C, 3 min), apparently increased the intraliposomal solution freezing exotherm of the suspensions containing the externally added glycerol or DMSO. Membrane disordering at and above the transition temperature should allow an influx of the highly permeable small solute molecules, and should, thus, reduce the osmotic effect that dehydrates the liposomes.

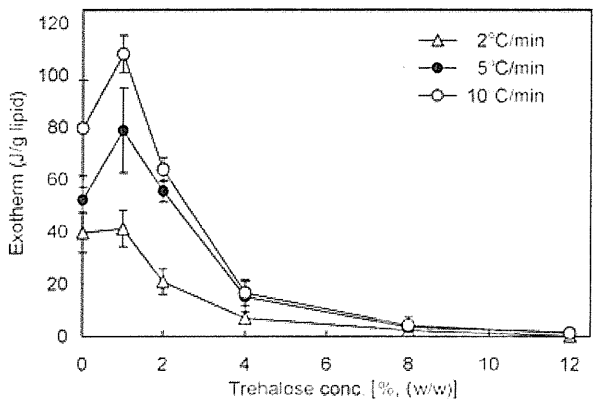

Figure 6. Effect of extraliposomal trehalose (0%–12%, w/w) on internal solution freezing exotherms of DPPC liposome suspensions (10 μL, 4% lipid in 10 mM Tris–HCl buffer, 0.2 μm) obtained by cooling at 2°C/min (△), 5°C/min (•), or 10°C/min (○)(average ± SD, $n = 3$).

The effect of intraliposomal trehalose on the freezing behavior of DPPC liposomes was also studied (Fig. 4a). The suspensions containing trehalose predominantly inside the liposomes showed apparently larger exotherms than those of other suspensions. The absence of the baseline shift at the trehalose transition temperature of maximally freeze-concentrated solutes (T_g') in the heating scan confirmed the low trehalose concentration outside the liposomes (data not shown). Liposomes prepared by extrusion often contain an amount of internal solution that was insufficient to fill the completely spherical structure, which allows inward water flow across the membrane upon exposure of liposomes to lower osmolarity solutions.[37] An increase in the intraliposomal solution content due to osmotic swelling in the initial suspension and limited freeze-induced dehydration can explain the larger ice formation peaks. These results indicated that the osmotic effect made a significant contribution to the freezing behavior of liposomes.

Kinetic stability of the trehalose-containing supercooled intraliposomal solutions was studied to elucidate their relevance in freeze-drying process (Fig. 8). Some liposome suspensions (e.g., trehalose-containing 0.8 μm DPPC liposome) showed small but apparent intraliposomal solution freezing peaks in the scans after a slower cooling (0.5°C/min) followed by being held at −35°C (180 min). The result suggested that some liposomes retain certain amount of internal solutions during freezing segment of pharmaceutical formulation lyophilization usually

DOI 10.1002/jps

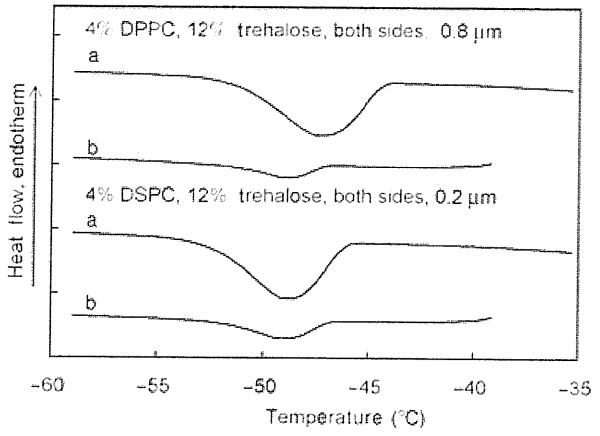

Figure 8. Cooling thermograms of DPPC (0.8 μm) and DSPC (0.2 μm) liposome suspensions containing trehalose (12%, w/w) on both sides of the membrane (10 μL, 4% lipids in 10 mM Tris–HCl buffer). The suspensions were cooled at 5°C/min (a) from room temperature or (b) after slow cooling (0.5°C/min) with a temporary pause at −35°C (180 min).

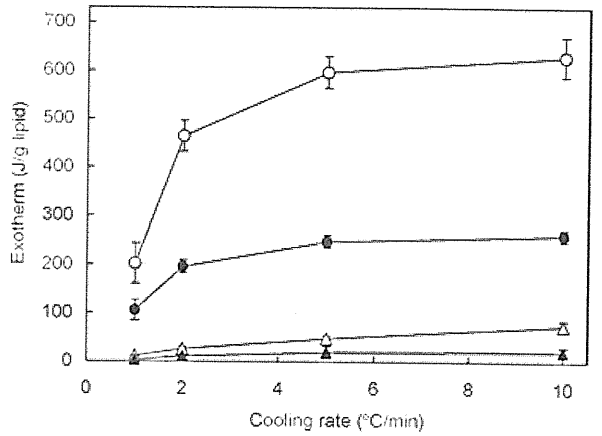

Figure 9. Internal solution freezing exotherms of carboxyfluorescein (25 mM)-containing DPPC liposome suspensions (10 μL, 4% DPPC in 10 mM Tris–HCl buffer, 0.2 μm) without (△) or with 12% trehalose on the outside (▲), inside (○), or both sides (●) of the liposome membrane scanned from room temperature at 1–10°C/min (average ± SD, $n = 3$).

performed via slow cooling (e.g., 0.2–0.5°C/min) down to −35°C to −50°C on the lyophilizer shelf.[38,39] The lower product temperature during the process should lead to freezing of the intraliposomal solutions by the homogeneous ice nucleation mechanism.

Effect of Freeze–Thawing on CF-Encapsulated Liposomes

The relationship between trehalose-induced changes in the liposome freezing behavior and functional stability of liposomes upon freeze–thawing was studied (Figs. 9 and 10). The CF-loaded DPPC liposomes were subjected to thermal analysis and freeze–thawing marker-retention study (a) without trehalose, (b) with trehalose on both sides of the membrane, (c) with trehalose in the intraliposomal solution, or (d) with trehalose in the extraliposomal media. A lower concentration (25 mM; approx. 0.94%, w/w) of CF compared with those in other retention studies (e.g., 100 mM) was used for the experiment to reduce its osmotic effect on the freezing behavior of the liposomes. A thermal transition ($T_g' = -36.2$°C) and absence of other peaks in the heating process of a frozen CF solution (25 mM in Tris–HCl buffer, pH 7.4) indicated that the solute was in a noncrystalline state in the freeze-concentrated phase. The CF-loaded liposome suspensions showed small intraliposomal solution freezing exotherms essentially identical to those of the marker-free samples in the absence of trehalose (Figs. 2 and 9). The liposomes lost a large fraction of the markers upon freeze–thawing of the trehalose-free suspensions cooled down to −35°C (below bulk solution freezing temperature) and −70°C (below intraliposomal solution freezing temperature) at all speeds (Fig. 10).

The DPPC liposomes containing trehalose on both sides of the membrane retained higher intraliposomal solution and encapsulated CF contents under faster cooling (5 and 10°C/min). Small changes of the marker retention in the fast cooling of the suspensions down to −35°C and −70°C suggested that the intraliposomal freezing by itself is not a main cause of the severe marker leakage, at least in the presence of trehalose. A large loss of the intraliposomal solution and

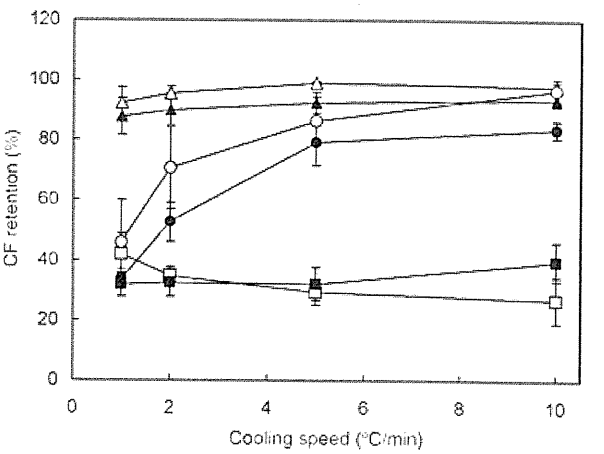

Figure 10. Effect of freeze–thawing on retention of carboxyfluorescein (CF) encapsulated in DPPC liposomes. Aliquots of CF (25 mM)-containing DPPC liposome suspension (10 μL, 4% lipid in 10 mM Tris–HCl buffer, 0.2 μm) without (□, ■) or with 12% trehalose on the outside (△, ▲) or both sides (○, ●) of the liposome membrane were cooled from room temperature to −35°C (open symbols) or −70°C (closed symbols) at 1–10°C/min, and then heated at 10°C/min (average ± SD, $n = 3$).

an accompanying apparent leakage of the marker in the slowly cooled suspensions suggested that membrane damage had occurred that allowed outbound flow of the marker-containing solution during the freezing process. Experiencing the fast-dehydrating temperature range twice in a freeze–thawing cycle should explain the larger change in marker retention compared with that of the intraliposomal freezing exotherm obtained in some cooling procedures. Suspensions containing CF and trehalose only in the intraliposomal solution also showed large intraliposomal solution freezing exotherms (Figs. 4a and 9). Solidification of the suspensions upon freeze–thawing, which hindered the CF retention measurement, confirmed the requirement of trehalose in the extraliposomal media (data not shown).[16]

The externally added trehalose (12%) reduced the CF leakage from the DPPC liposomes upon freeze–thawing at all cooling speeds. The suspensions showed a minor exotherm during the intraliposomal solution freezing. Possible osmotic shrinkage prior to freezing is the likely explanation for the limited internal solution content and the high retention of the encapsulated marker.[4,22,26] The addition of trehalose to the extraliposomal media (12%) induced leakage of less than 1% of the encapsulated CF at room temperature (data not shown).[40] Changes in the color of CF-containing liposome suspensions from yellow to orange by the extraliposomal trehalose suggested an increasing intraliposomal marker concentration due to outbound water flow through membrane diffusion (osmotic shrinkage). The lower intraliposomal solution contents should lead to the limited freeze-induced dehydration and membrane damage. The extraliposomal saccharides should also protect liposomes from membrane injury due to the growing ice surface, an excess concentration of unfavorable solutes (e.g., inorganic salts), and direct contact of concentrated liposome membranes as spacer.[40,39]

Liposome Stabilization by Control of the Osmotic Flow and Internal Freezing

The results indicated varied effect of trehalose on the freezing behavior and functional stability of liposomes upon freeze–thawing depending on its distribution across the membrane. A schematic flow of the liposome freezing behavior is shown in Figure 11. Understanding the physical changes and the encountering stresses should be relevant for strategic stabilization in freeze–thawing and freeze-drying of liposomes. Liposomes prepared by extrusion often do not contain sufficient solutions to fill the spherical structure.[37,41] Exposure of the liposomes either increases (e.g., osmotic swelling in hypotonic media) or decreases (e.g., osmotic shrinkage in hypertonic media) the internal solution content via water diffusion through the membranes. The bulk and intraliposomal solutions freeze at different temperatures, as the processes are initiated by the heterogeneous and homogeneous ice nucleation mechanisms, respectively. The freeze-induced osmotic dehydration and the intraliposomal solution freezing initiated by membrane-penetrating ice crystals should reduce intraliposomal solution content that freeze at the homogeneous ice nucleation temperature.[12,16,34,42] Accordingly, the intraliposomal solution should be in the dehydrated, supercooled, or frozen states in the frozen suspensions depending on the formulation and process factors. The absence of crystallizing solutes (e.g., mannitol) allowed observation of the freeze-induced physical changes through thermal analysis.[28]

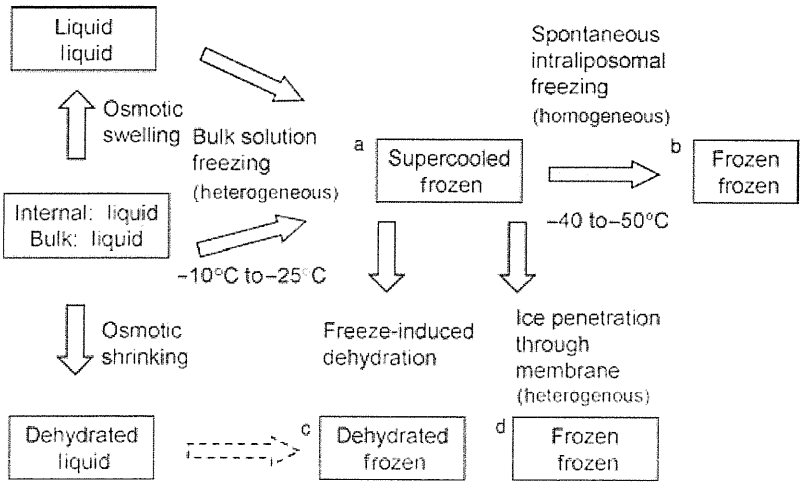

Figure 11. Schematic freezing behaviors of extruded liposome suspensions. The upper and lower rows in each box denote the physical state of the intraliposomal and bulk solutions, respectively. Boxes (a) to (d) indicate suggested physical states of frozen liposome suspensions.

DOI 10.1002/jps

Each step of the freeze-related physical changes induces stresses that affect the stability of liposomes. The growing ice during the bulk and intraliposomal solution freezing should physically damage the liposome membranes. It is possible that the freeze-induced large difference in the osmotic pressure causes larger membrane damage in the DPPC liposomes than in the living cells because of their lower hydraulic permeability, leading to a dehydrating flow of the CF-containing intraliposomal solutions. The liposomes should also experience stresses by ice crystal size growth (Ostwald ripening) and rapid dilution of the surrounding media during the thawing process of the frozen suspensions.[23,43]

The different stability-determining factors during the freezing process of the marker-loaded liposomes from those of the living cells suggest requirement of different strategies for their stabilization.[44] Trehalose protected the marker-loaded liposomes through two types of osmotic effects that prevent the freeze-induced internal solution loss during freeze–thawing. The addition of trehalose to both sides of the liposome membrane prevented both the freeze-induced dehydration and water-soluble marker loss, particularly in the higher cooling rate. The marker retention was also achieved by extraliposomal trehalose that osmotically dehydrates the liposomes through outbound water diffusion without apparent CF release in the initial suspensions. The prior dehydration should prevent the freeze-induced membrane damage even in the slower cooling. These osmotic effects should contribute as one of the major mechanisms by which trehalose protects liposomes during the freezing process besides the water-substitution, bulking, and molecular mobility reduction. The liposomes containing sufficiently high concentrations of cryoprotectants can be vitrified without the apparent ice formation by ultrafast cooling (e.g., immersion of small volume suspensions in liquid nitrogen). The vitrification method would not be practical for large-scale freezing of liposome formulations, although it is a popular way to avoid intracellular freezing during cryopreservation of living cells.[12] Formulation and process optimization of liposome pharmaceuticals should be performed through multiple assay methods (e.g., API retention, liposome fusion, aggregation, and activity of encapsulated enzyme) that appropriately detect the changes caused by different stresses.

The varied physical states of the intraliposomal solutions in the frozen suspensions should directly (e.g., membrane damage due to ice growth) or indirectly (e.g., altered excipient–membrane interactions) affect the liposome stability during freeze-drying process and subsequent storage.[1,5,8,45] The trehalose molecules are required to be distributed in the position spatially accessible to the membrane phospholipids to form the water-substituting interactions that protect the membrane structure from the dehydration stresses. The higher glass transition temperatures (T_g) of the dried solids and resistance against changes by absorbed water should make trehalose a potent stabilizer for lyophilization and subsequent storage of liposomes and biomacromolecules.[39] How the altered freezing behavior affects liposome stability during freeze-drying is an intriguing topic for further study.

The present results indicate the relevance of characterizing the freeze-related physical changes of liposomes for the development of frozen or freeze-dried formulations. The liposome composition and trehalose distribution across the membrane significantly affected the osmotic solution flows that determine the physical states of their intraliposomal solutions and functional stabilities (e.g., CF retention) upon freeze–thawing. Potentially varied molecular interactions between components would also affect liposome stability in the subsequent drying process and in storage. Controlling the osmotically mediated physical changes through formulation design and process optimization would be valuable in the cryopreservation and freeze-drying of liposome pharmaceuticals.

REFERENCES

1. Chen C, Han D, Cai C, Tang X. 2010. An overview of liposome lyophilization and its future potential. J Control Release 142:299–311.
2. Misra A, Jinturkar K, Patel D, Lalani J, Chougule M. 2009. Recent advances in liposomal dry powder formulations: Preparation and evaluation. Expert Opin Drug Deliv 6:71–89.
3. van Winden EC. 2003. Freeze-drying of liposomes: Theory and practice. Methods Enzymol 367:99–110.
4. Wessman P, Edwards K, Mahlin D. 2010. Structural effects caused by spray- and freeze-drying of liposomes and bilayer disks. J Pharm Sci 99:2032–2048.
5. Nakagaki M, Nagase H, Ueda H. 1992. Stabilization of the lamellar structure of phosphatidylcholine by complex formation with trehalose. J Memb Sci 73:173–180.
6. Crowe JH, Crowe LM, Chapman D. 1984. Preservation of membranes in anhydrobiotic organisms: The role of trehalose. Science 223:701–703.
7. Ausborn M, Schreierb H, Brezesinskic G, Fabiand H, Meyere HW, Nuhna P. 1994. The protective effect of free and membrane-bound cryoprotectants during freezing and freeze-drying of liposomes. J Control Release 30:105–116.
8. Crowe JH, Crowe LM, Carpenter JF, Rudolph AS, Wistrom CA, Spargo BJ, Anchordoguy TJ. 1988. Interactions of sugars with membranes. Biochim Biophys Acta 947:367–384.
9. Wolfe J, Bryant G. 1999. Freezing, drying, and/or vitrification of membrane-solute-water systems. Cryobiology 39:103–129.
10. Lovelock JE. 1954. The protective action of neutral solutes against haemolysis by freezing and thawing. Biochem J 56:265–270.
11. Rasmussen DH, Macaulay MN, MacKenzie AP. 1975. Supercooling and nucleation of ice in single cells. Cryobiology 12:328–339.
12. Mazur P. 1984. Freezing of living cells: Mechanisms and implications. Am J Physiol 247:C125–C142.

13. Shirakashi R, Tanasawa I. 1998. Method of designing prefreezing protocol in cryopreservation of biological materials. Ann N Y Acad Sci 858:175–182.
14. Mathias SF, Franks F, Hatley RH. 1985. Preservation of viable cells in the undercooled state. Cryobiology 22:537–546.
15. Siow LF, Rades T, Lim MH. 2007. Characterizing the freezing behavior of liposomes as a tool to understand the cryopreservation procedures. Cryobiology 55:210–221.
16. Siow LF, Rades T, Lim MH. 2008. Cryo-responses of two types of large unilamellar vesicles in the presence of non-permeable or permeable cryoprotecting agents. Cryobiology 57:276–285.
17. Talsma H, Van Steenbergen MJ, Crommelin DJ. 1992. The cryopreservation of liposomes. 2. Effect of particle size on crystallization behavior and marker retention. Cryobiology 29:80–86.
18. Charoenrein S, Reid DS. 1989. The use of DSC to study the kinetics of heterogeneous and homogeneous nucleation of ice in aqueous systems. Thermochim Acta 156:373–381.
19. Seki S, Kleinhans FW, Mazur P. 2009. Intracellular ice formation in yeast cells vs. cooling rate: Predictions from modeling vs. experimental observations by differential scanning calorimetry. Cryobiology 58:157–165.
20. Bronshteyn VL, Steponkus PL. 1993. Calorimetric studies of freeze-induced dehydration of phospholipids. Biophys J 65:1853–1865.
21. Lefevre T, Toscani S, Picquart M, Dugue J. 2002. Crystallization of water in multilamellar vesicles. Eur Biophys J 31:126–135.
22. Siminovitch D, Chapman D. 1971. Liposome bilayer model systems of freezing living cells. FEBS Lett 16:207–212.
23. Talsma H, Steenbergen MJV, Crommelin DJA. 1991. The cryopreservation of liposomes: 3. Almost complete retention of a water-soluble marker in small liposomes in a cryoprotectant containing dispersion after a freezing/thawing cycle. Int J Pharm 77:119–126.
24. Harrigan PR, Madden TD, Cullis PR. 1990. Protection of liposomes during dehydration or freezing. Chem Phys Lipids 52:139–149.
25. Higgins J, Hodges NA, Olliff CJ, Phillips AJ. 1986. Factors influencing cryoprotective activity and drug leakage from liposomes after freezing. J Pharm Pharmacol 38:259–263.
26. Hupfeld S, Moen HH, Ausbacher D, Haas H, Brandl M. 2010. Liposome fractionation and size analysis by asymmetrical flow field-flow fractionation/multi-angle light scattering: Influence of ionic strength and osmotic pressure of the carrier liquid. Chem Phys Lipids 163:141–147.
27. Ohtake S, Schebor C, Palecek SP, de Pablo JJ. 2005. Phase behavior of freeze-dried phospholipid-cholesterol mixtures stabilized with trehalose. Biochim Biophys Acta 1713:57–64.
28. Talsma H, van Steenbergen MJ, Salemink PJ, Crommelin DJ. 1991. The cryopreservation of liposomes. 1. A differential scanning calorimetry study of the thermal behavior of a liposome dispersion containing mannitol during freezing/thawing. Pharm Res 8:1021–1026.
29. MacDonald RC, MacDonald RI, Menco BP, Takeshita K, Subbarao NK, Hu LR. 1991. Small-volume extrusion apparatus for preparation of large, unilamellar vesicles. Biochim Biophys Acta 1061:297–303.
30. Kristiansen J. 1992. Leakage of a trapped fluorescent marker from liposomes: Effects of eutectic crystallization of NaCl and internal freezing. Cryobiology 29:575–584.
31. Bartlett GR. 1959. Phosphorus assay in column chromatography. J Biol Chem 234:466–468.
32. Kaasgaard T, Mouritsen OG, Jørgensen K. 2003. Freeze/thaw effects on lipid-bilayer vesicles investigated by differential scanning calorimetry. Biochim Biophys Acta 1615:77–83.
33. Wu WG, Chi LM, Yang TS, Fang SY. 1991. Freezing of phosphocholine headgroup in fully hydrated sphingomyelin bilayers and its effect on the dynamics of nonfreezable water at subzero temperatures. J Biol Chem 266:13602–13606.
34. Rall WF, Mazur P, McGrath JJ. 1983. Depression of the ice-nucleation temperature of rapidly cooled mouse embryos by glycerol and dimethyl sulfoxide. Biophys J 41:1–12.
35. Nagle JF, Wilkinson DA. 1978. Lecithin bilayers. Density measurement and molecular interactions. Biophys J 23:159–319.
36. Koster KL, Lei YP, Anderson M, Martin S, Bryant G. 2000. Effects of vitrified and nonvitrified sugars on phosphatidylcholine fluid-to-gel phase transitions. Biophys J 78:1932–1946.
37. Mui BL, Cullis PR, Evans EA, Madden TD. 1993. Osmotic properties of large unilamellar vesicles prepared by extrusion. Biophys J 64:443–453.
38. Akers MJ, Vasudevan V, Stickelmeyer M. 2002. Formulation development of protein dosage forms. Pharm Biotechnol 14:47–127.
39. Nail SL, Jiang S, Chongprasert S, Knopp SA. 2002. Fundamentals of freeze-drying. Pharm Biotechnol 14:281–360.
40. Blok MC, van Deenen LL, De Gier J. 1976. Effect of the gel to liquid crystalline phase transition on the osmotic behaviour of phosphatidylcholine liposomes. Biochim Biophys Acta 433:1–12.
41. Pencer J, White GF, Hallett FR. 2001. Osmotically induced shape changes of large unilamellar vesicles measured by dynamic light scattering. Biophys J 81:2716–2728.
42. Suzuki T, Komatsu H, Miyajima K. 1996. Effects of glucose and its oligomers on the stability of freeze-dried liposomes. Biochim Biophys Acta 1278:176–182.
43. Grabielle-Madelmont C, Perron R. 1983. Calorimetric studies on phospholipid-water systems: II. Study of water behavior. J Colloid Interface Sci 95:483–493.
44. Hubel A, Darr TB, Chang A, Dantzig J. 2007. Cell partitioning during the directional solidification of trehalose solutions. Cryobiology 55:182–188.
45. Ohtake S, Schebor C, de Pablo JJ. 2006. Effects of trehalose on the phase behavior of DPPC-cholesterol unilamellar vesicles. Biochim Biophys Acta 1758:65–73.

DOI 10.1002/jps